

Compound and perpendicular diffusion of cosmic rays and random walk of the field lines: II.
Non-parallel particle transport and drifts

This article has been downloaded from IOPscience. Please scroll down to see the full text article.

2009 J. Phys. A: Math. Theor. 42 235502

(<http://iopscience.iop.org/1751-8121/42/23/235502>)

View [the table of contents for this issue](#), or go to the [journal homepage](#) for more

Download details:

IP Address: 171.66.16.154

The article was downloaded on 03/06/2010 at 07:52

Please note that [terms and conditions apply](#).

Compound and perpendicular diffusion of cosmic rays and random walk of the field lines: II. Non-parallel particle transport and drifts

G M Webb¹, E Kh Kaghshvili², J A le Roux^{1,3}, A Shalchi^{4,5},
G P Zank^{1,3} and G Li^{1,3}

¹ CSPAR, University of Alabama Huntsville, Huntsville AL 35805, USA

² Atmospheric and Environmental Research Inc., Lexington, MA 02421-3126, USA

³ Department of Physics, University of Alabama, Huntsville, Huntsville AL 35899, USA

⁴ Institut für Theoretische Physik, Lehrstuhl IV: Weltraum und Astrophysik, Ruhr Universität, D-44780 Bochum, Germany

E-mail: gmwebb@cspar.uah.edu

Received 9 February 2009, in final form 24 April 2009

Published 22 May 2009

Online at stacks.iop.org/JPhysA/42/235502

Abstract

Compound transport of energetic charged particles across the mean magnetic field due to field line random walk is investigated by means of a Chapman–Kolmogorov equation. The probability distribution function (pdf) for the particle transport across the field P_{\perp} is given as a convolution of the pdf for random walk of the magnetic field, P_{FRW} , with the pdf P_p , for particle transport relative to the random walking field. The particle propagator P_p includes the effects of advection, drift, parallel diffusion and local perpendicular diffusion of particles relative to the random walking field. At early times, the particles sub-diffuse across the field due to field line random walk. At late times, the effective cross-field diffusion coefficient has the form $\kappa_{\perp e} = \kappa_{\perp} + \kappa_F$. The diffusion coefficient κ_{\perp} is the local cross-field diffusion coefficient due to particle scattering in the random magnetic field. The diffusion coefficient κ_F is due to coherent particle advection parallel to the mean magnetic field \mathbf{B}_0 coupled with transverse random walk of the magnetic field. Estimates of cross-field diffusion due to field line random walk, advection and drift are obtained both near to the heliospheric current sheet at Earth and at higher helio-latitudes. Cross-field diffusion due to field line random walk and advection is shown to be an important transport mechanism for low-energy particles near the current sheet, where the effects of drifts are negligible. Drift effects and field line random walk are also assessed at higher helio-latitudes off the current sheet, for a model interplanetary magnetic field, with a flat current sheet in the helio-equatorial plane.

⁵ Work carried out at CSPAR, Huntsville AL 35805, USA.

PACS numbers: 96.50.S, 96.50.Sh, 94.05.Lk, 96.50.Bh, 05.40.—a

(Some figures in this article are in colour only in the electronic version)

1. Introduction

Field line random walk is a subject of widespread interest and application in space plasma physics and in fusion plasmas (e.g., Jokipii and Parker (1969), Jokipii (1973), Krommes *et al* (1983), Matthaeus *et al* (1995), Isichenko (1991a, 1991b), Barghouty and Jokipii (1996), Ragot (1999, 2000, 2006a–2006f, 2009), Shalchi and Kourakis (2007a, 2007b), Shalchi *et al* (2007), Shalchi and Weinhorst (2009), Chuychai *et al* (2005), Zimbardo *et al* (2000, 2004), Ruffolo *et al* (2003, 2004, 2006)). Matthaeus *et al* (1995) invoked Corsinn's independence hypothesis (Corsinn 1959) to determine the form of the field line random walk coefficient for 2D plus slab turbulence, assuming that the integrals involved in the theory converged. Ragot (1999, 2001) showed that the mean square perpendicular deviation of the field line random walk $\langle \Delta x^2 \rangle \propto |\Delta z|^\alpha$ could be normal ($\alpha = 1$), superdiffusive ($\alpha > 1$) or subdiffusive ($\alpha < 1$) depending on the shape of the power spectrum of the turbulent magnetic field (see also later papers by Ragot *et al* (2006a–2006c) and Shalchi and Kourakis (2007a, 2007b)). These results are in general important in determining the cross-field transport of energetic charged particles due to field line random walk.

The quasilinear theory for cosmic ray diffusion in weak slab turbulence was developed by Jokipii (1966), Hasselman and Wibberenz (1968) and Hall and Sturrock (1967) (see also the review by Jokipii (1971)). The spatial diffusion coefficient for particle transport parallel to the mean magnetic field κ_{\parallel} , and the pitch angle diffusion coefficient for particles $D_{\mu\mu}$ (μ denotes the particle pitch angle cosine), obtained in these analyses depends on the power in the magnetic turbulence in cyclotron resonance with the particles. The perpendicular spatial diffusion coefficient κ_{\perp} is proportional to the power in the turbulence at zero wave number associated with random walk of the field lines (e.g., Jokipii (1966), Jokipii and Parker (1969), Forman *et al* (1974)). Forman *et al* (1974) gave a unified kinetic theory derivation of the perpendicular and parallel diffusion coefficients κ_{\perp} and κ_{\parallel} as well as the anti-symmetric components of the diffusion tensor, κ_A , associated with particle drifts for the case of weak slab turbulence (for a recent account of quasilinear theory, see e.g. Schlickeiser 2001).

However, numerical simulations of charged particle transport in random magnetic fields (Giacalone and Jokipii (1999), Mace *et al* (2000) and Qin *et al* (2002a, 2002b, 2003)) have revealed that the quasilinear theory for spatial diffusion of cosmic rays perpendicular to the mean magnetic field does not adequately account for the results of the simulations. Theoretical work by Matthaeus *et al* (2003), Zank *et al* (2004) and Shalchi *et al* (2004) provides a more satisfactory account for the results of the numerical simulations and in particular the dependence of κ_{\perp} on the particle gyro-radius r_g . In particular, κ_{\perp} is given by a nonlinear integral equation involving an integral over the turbulence spectrum, which is assumed to be a combination of slab plus 2D turbulence. This nonlinear guiding center theory (NLGC theory) is based on the transverse motion of the particle gyro-center due to the random magnetic field, and in addition, the particle moves diffusively along its orbit as it samples the random magnetic field correlations, rather than along the quasilinear orbit.

Webb *et al* (2006) (hereinafter referred to as paper I) presented an analysis of compound transport of cosmic rays across a random walking magnetic field, in which the probability distribution function (pdf) $P_{\perp}(x, y, t|x_0, y_0, t_0)$ for particles to cross the mean field is given by

a Chapman–Kolmogorov equation, (e.g. Gardiner 1985) where the mean field $\langle \mathbf{B} \rangle$ is along the z -axis. The pdf P_{\perp} is given as the convolution of the probability distribution $P_{p\parallel}(z, t|z_0, t_0)$ for the particle to move a distance $\Delta z = z - z_0$ along the mean field in a time $\Delta t = t - t_0$, and the pdf $P_{\text{FRW}}(x, y|z)$ is the random walking field consists of a step $\Delta \mathbf{x}_{\perp} = (x - x_0, y - y_0, 0)$ across the mean field direction corresponding to a step $\Delta z = z - z_0$ along the field. In this model, the particle is trapped on the random walking field line. The field line random walk statistics governed by $P_{\text{FRW}}(x, y|z)$ was taken as a Gaussian distribution with diffusion coefficient $D_L = \langle (\Delta x)^2 / (2\Delta z) \rangle = \langle (\Delta y)^2 / (2\Delta z) \rangle$.

The origin of the so-called ‘dropouts’ observed in the low energy solar cosmic ray intensity (~ 20 keV–2 MeV H–Fe ions) observed by the ACE spacecraft (Mazur *et al* 2000) provided a challenge to theoretical cross-field diffusion theory. Theoretical models of the dropouts were proposed by Giacalone *et al* (2000), Zimbardo *et al* (2004), Ruffolo *et al* (2003), Kaghshvili *et al* (2006) and Webb *et al* (2006). Webb *et al* (2006) studied the nature of cross-field transport due to compound diffusion (also known as subdiffusion). Compound diffusion has been inferred to occur in simulations of cross-field particle transport in slab turbulence (Mace *et al* (2000), Qin *et al* (2002a, 2002b, 2003)). Shalchi (2005) used nonlinear guiding center theory (NLGC theory) to obtain the subdiffusive result $\langle \Delta x_{\perp}^2 \rangle \propto (\Delta t)^{1/2}$ for particle transport across the mean magnetic field $\langle \mathbf{B} \rangle$ in slab turbulence, which provides a theoretical explanation of the simulations.

In this paper we extend the results of paper I, by allowing a more general propagator, P_p , for particle propagation along and perpendicular to the local field. In particular, we consider models for P_p that allow the particles to both drift along and perpendicular to the local field, and also to diffuse across the random walking field. As in paper I, the probability distribution $P_{\perp}(x, y, t|x_0, y_0, t_0)$ is given as a convolution of the particle propagator P_p with the probability distribution $P_{\text{FRW}}(x, y|z)$ describing the field line random walk. A brief account of this model is given in Webb *et al* (2008). We find that at early times, the particles undergo compound diffusion, with $\langle \Delta x_{\perp}^2 \rangle \propto \Delta t^{1/2}$, but at late times, the particles have an effective cross-field diffusion coefficient $\kappa_{\perp e} = \kappa_{\perp} + \kappa_F$. The diffusion coefficient κ_{\perp} is the local cross-field diffusion coefficient due to particle scattering in the random magnetic field. The diffusion coefficient $\kappa_F = |V_z|D_L$, where $|V_z|$ is the net advection speed of the particles in bulk along the mean field and $D_L = \langle \Delta x^2 / 2\Delta z \rangle$ is the field line random walk coefficient (x denotes the distance across the mean field and z denotes the distance along the mean field). Our expression for κ_F is similar to the perpendicular diffusion coefficient for field line random walk obtained by Jokipii (1966) and Jokipii and Parker (1969), except that in their theory, V_z is replaced by the particle speed along the field. The diffusion of particles across a random walking magnetic field is somewhat analogous to the transverse spreading of water drops in a garden hose in which there is a high-speed water jet passing through the hose when the water is turned on. The fire hose instability causes the hose to writhe sideways. The analogy is not precise. Our result for κ_F is similar to that of Chuvilgin and Ptuskin (1993), who studied particle transport in a random magnetic field, with multiple scales (in their case the effective bulk velocity can be identified with the Alfvén speed plus an effective drift speed).

Shalchi *et al* (2009a) explore the role of field line random walk and advection, drifts and wave propagation effects on the cross-field transport of particles, with similar results to this paper. They give an extensive description of the statistics of the field line random walk $\langle \Delta x^2 \rangle \propto |\Delta z|^{\alpha}$ for the second moment for slab plus 2D turbulence and concentrate on the second moment of the pdf P_{\perp} . Our paper concentrates more on a generalized form of the Chapman–Kolmogorov equation for cross-field transport and a detailed description of P_{\perp} not addressed by Shalchi *et al* (2009a).

Section 2 develops the Chapman–Kolmogorov transport equation for cross-field particle transport in which P_p is described by an advection–diffusion equation for the particle transport relative to the random walking field. The form of the Chapman–Kolmogorov equation for P_\perp is significantly more complicated than in paper I, since P_p now allows for transport of particles perpendicular to the random walking magnetic field as well as the effects of drifts. The Laplace–Fourier transform form of P_\perp is determined and used to delineate the late time, long space scale behavior of P_\perp . It is also used to determine the short time and short space scale behavior of P_\perp . At late times, P_\perp satisfies an advection–diffusion equation, including an enhanced cross-field diffusion of particles due to field line random walk and due to drifts and advection parallel to the mean magnetic field as well as a fourth-order diffusion term associated with compound diffusion. At early times, P_\perp satisfies a fractional Fokker–Planck equation describing compound diffusion. The general form of the fractional Fokker–Planck equation is determined by Fourier–Laplace inversion. A Hankel transform formulation of the solution reduces the formula for P_\perp to a one-dimensional integral over the position coordinate z along the field line, which reveals the intimate connection between field line random walk and cross-field diffusion (see equation (2.64)). The moments of the probability distribution P_\perp are investigated and the lower order moments are studied in detail. Section 3 presents numerical solutions for P_\perp and discusses the form of P_\perp for different values of the parameters, including the limit of compound diffusion studied by Webb *et al* (2006). Section 4 discusses the role of enhanced cross-field diffusion due to field line random walk, and advection and drift parallel to the mean field, and possible applications to the eleven year solar cycle modulation of galactic cosmic rays. Section 5 concludes with a summary and discussion.

2. Three-dimensional diffusion and drift

In paper I, compound diffusion of particles due to random walk of the magnetic field lines was modeled using the Chapman–Kolmogorov equation:

$$P_\perp(x, y, t|x_0, y_0, t_0) = \int_{-\infty}^{\infty} dz P_{\text{FRW}}(x, y|z; x_0, y_0, z_0) P_{p\parallel}(z, t|z_0, t_0), \quad (2.1)$$

where $P_\perp(x, y, t|x_0, y_0, t_0)$ is the probability that the particle moves a step $\Delta\mathbf{x}_\perp = (x - x_0, y - y_0, 0)$ across the mean magnetic field (assumed to lie along the z -axis) in a time $\Delta t = t - t_0$, P_{FRW} is the probability that the random field consists of a step Δx normal to the mean magnetic field corresponding to a step $\Delta z = z - z_0$ along the field and $P_{p\parallel}(z, t|z_0, t_0)$ gives the probability that the particle will move a distance Δz along the field in a time Δt .

In this paper, (2.1) is replaced by the generalized Chapman–Kolmogorov equation

$$P_\perp(x, y, t|x_0, y_0, t_0) = \int_{-\infty}^{\infty} dx_1 \int_{-\infty}^{\infty} dy_1 \int_{-\infty}^{\infty} dz P_{\text{FRW}}(x_1, y_1|z; x_0, y_0, z_0) \\ \times P_p(x, y, z, t|x_1, y_1, z_0, t_0), \quad (2.2)$$

which consists of the convolution of the field line random walk probability P_{FRW} and the particle probability density P_p describing the transport of the particle relative to the random walking field line. In (2.2), account is taken of the transport of particles across the random walking field, in moving from (x_1, y_1, z) , the location on the field line, to the particle position at (x, y, z) due to cross-field transport of the particles. The case of pure parallel transport of particles along the field described by (2.1) is recovered if $P_p = P_{p\parallel}\delta(x - x_1)\delta(y - y_1)$ in (2.2).

2.1. The model

The fundamental diffusive transport equation for cosmic rays in space plasmas, describing convection, anisotropic diffusion, particle drifts and adiabatic energy changes, was originally derived by Parker (1965) (see also Krymsky 1964). Further derivations of the equation, including the effects of second-order Fermi acceleration, and different equivalent forms of the equation, emphasizing different aspects of the physics, were obtained by Dolginov and Toptygin (1967, 1968), Gleeson and Axford (1967), Jokipii and Parker (1970), Skilling (1975), Webb and Gleeson (1979), Webb (1985, 1989), Earl *et al* (1988) and others. The transport equation neglecting the effects of second-order Fermi acceleration can be written in the form

$$\frac{\partial f}{\partial t} + (\mathbf{u} + \mathbf{V}_D) \cdot \nabla f - \nabla \cdot (\mathbf{K}^{(s)} \cdot \nabla f) - \frac{p}{3} \nabla \cdot \mathbf{u} \frac{\partial f}{\partial p} = 0, \quad (2.3)$$

where f is the isotropic momentum–space distribution function for the energetic particles, $\mathbf{K}^{(s)}$ is the symmetric part of the cosmic ray diffusion tensor representing particle transport due to diffusion parallel (κ_{\parallel}) and perpendicular (κ_{\perp}) to the mean magnetic field, \mathbf{u} is the velocity of the background plasma, and \mathbf{V}_D is the effective drift velocity of the particles due to curvature and gradient drifts, and drifts parallel to the mean magnetic field. The drift velocity \mathbf{V}_D is given by

$$\mathbf{V}_D = \nabla \times (\kappa_A \mathbf{e}_B), \quad (2.4)$$

where $\mathbf{e}_B = \mathbf{B}/B$ is the unit vector along the mean magnetic field \mathbf{B} . The drift velocity \mathbf{V}_D has zero divergence ($\nabla \cdot \mathbf{V}_D = 0$), and in the weak scattering limit, $\kappa_A \simeq vr_L/3$ where v is the particle speed and $r_L = pc/ZeB$ is the particle Larmor-radius, p is the particle momentum, Ze the particle charge and c is the speed of light. In this limit, the drift velocity is equivalent to that expected for a near isotropic distribution of particles in adiabatic, guiding center drift theory (e.g., Kota (1979), Webb *et al* (1981), Burger *et al* (1985)). The drift velocity \mathbf{V}_D can be decomposed into components parallel ($\mathbf{V}_{D\parallel}$) and perpendicular ($\mathbf{V}_{D\perp}$) to the mean magnetic field in the form

$$\mathbf{V}_D = \mathbf{V}_{D\perp} + \mathbf{V}_{D\parallel}, \quad (2.5)$$

where

$$\mathbf{V}_{D\parallel} = \frac{\kappa_A}{B} \nabla \times \mathbf{B} \cdot \mathbf{e}_B \mathbf{e}_B, \quad \mathbf{V}_{D\perp} = \mathbf{V}_D - \mathbf{V}_{D\parallel}, \quad (2.6)$$

where \mathbf{e}_B is the unit vector along the magnetic field \mathbf{B} . In (2.6), $\mathbf{V}_{D\perp}$ is due to curvature and gradient drifts (more generally the curvature drift is part of the so-called acceleration drift). The particle velocity parallel to the magnetic field in drift theory consists of the component of the particle velocity at the particle position parallel to the magnetic field, namely $v \cos \theta$ (θ is the particle pitch angle) plus a component $vr_L \sin^2 \theta \nabla \times \mathbf{B}/(2B) \mathbf{e}_B$ due to the difference in the position of the guiding center and the particle in its orbit about the gyro-center. The average of the latter term over a near isotropic pitch angle distribution gives the result for $\mathbf{V}_{D\parallel}$ in (2.6) with $\kappa_A = vr_L/3$ appropriate for the weak scattering limit.

Below we consider a simplified analytical model of particle transport in a random walking magnetic field, including the effects of anisotropic diffusion of particles parallel and perpendicular to \mathbf{B} , and including the effects of particle drifts. If we neglect the effects of adiabatic energy changes in the Parker equation (2.3) and assume for analytical simplicity that \mathbf{V}_D and $\mathbf{K}^{(s)}$ can be regarded as constants, then (2.3) assumes the form

$$\frac{\partial f}{\partial t} + \mathbf{V} \cdot \nabla f - \kappa_{\parallel} \frac{\partial^2 f}{\partial z^2} - \kappa_{\perp} \left(\frac{\partial^2 f}{\partial x^2} + \frac{\partial^2 f}{\partial y^2} \right) = 0, \quad (2.7)$$

where $\mathbf{V} = \mathbf{u} + \mathbf{V}_D$ is the total advection speed due to both the plasma bulk velocity \mathbf{u} and the drift velocity \mathbf{V}_D . Here the z -axis is along the mean magnetic field and the x - and y -axes are orthogonal to \mathbf{B} . The Chapman–Kolmogorov-type equation for particle transport in a random walking magnetic field analogous to (2.1) is

$$P_{\perp}(x, y, t|x_0, y_0, t_0) = \int_{-\infty}^{\infty} dx_1 \int_{-\infty}^{\infty} dy_1 \int_{-\infty}^{\infty} dz P_{\text{FRW}}(x_1, y_1|z) \times P_{p\parallel}(z, t|z_0, t_0) P_{p\perp}(x, y, t|x_1, y_1, t_0), \quad (2.8)$$

where

$$P_{\text{FRW}}(x_1, y_1|z) = \frac{1}{4\pi D_L |z - z_0|} \exp\left(-\frac{(x_1 - x_0)^2 + (y_1 - y_0)^2}{4D_L |z - z_0|}\right) \quad (2.9)$$

is the probability distribution describing the field line random walk. The probability distribution

$$P_{p\parallel}(z, t|z_0, t_0) = \frac{1}{(4\pi\kappa_{\parallel}\Delta t)^{1/2}} \exp\left(-\frac{(z - z_0 - V_z\Delta t)^2}{4\kappa_{\parallel}\Delta t}\right) H(\Delta t), \quad (2.10)$$

where $\Delta t = t - t_0$, describes particle transport parallel to the mean magnetic field. The probability distribution

$$P_{p\perp}(x, y, t|x_1, y_1, t_0) = \frac{1}{4\pi\kappa_{\perp}\Delta t} \exp\left(-\frac{(x - x_1 - V_x\Delta t)^2 + (y - y_1 - V_y\Delta t)^2}{4\kappa_{\perp}\Delta t}\right) \quad (2.11)$$

describes particle transport perpendicular to \mathbf{B}_0 . Note that the probability distribution $P_p = P_{p\parallel}P_{p\perp}$ obtained from (2.10) and (2.11) is the Green’s function of the drift–advection–diffusion equation (2.7).

It is of interest to note that

$$\lim_{\kappa_{\parallel}\Delta t \rightarrow 0} P_{p\parallel}(z, t|z_0, t_0) = \delta(z - z_0 - V_z\Delta t), \quad (2.12)$$

$$\lim_{\kappa_{\perp}\Delta t \rightarrow 0} P_{p\perp}(x, y, t|x_1, y_1, t_0) = \delta(x - x_1 - V_x\Delta t)\delta(y - y_1 - V_y\Delta t). \quad (2.13)$$

In particular, if $V_x = 0$ and $V_y = 0$, then taking the limit as $\kappa_{\perp} \rightarrow 0$ and using (2.13) in (2.8) we recover the case where the particles are tied to the field lines and there is no cross-field drift. The limiting cases $\kappa_{\parallel}\Delta t \rightarrow 0$ and $\kappa_{\perp}\Delta t \rightarrow 0$ in (2.12) and (2.13) suggest that drift effects are similar in some respects to the ballistic transport case described by the telegrapher equation propagator (see Webb *et al* (2006)), in that both models give rise to cross-field diffusion due to field line random walk and non-stochastic particle motion along the field.

2.2. Probability distribution and Fourier–Laplace transforms

In the analysis of the probability distribution (2.8), it is convenient to use the transverse position coordinates

$$\tilde{x} = x - x_0 - V_x\Delta t, \quad \tilde{y} = y - y_0 - V_y\Delta t \quad (2.14)$$

and the corresponding polar coordinates (\tilde{r}, ϕ) , where

$$\tilde{x} = \tilde{r} \cos \phi, \quad \tilde{y} = \tilde{r} \sin \phi. \quad (2.15)$$

In terms of these coordinates, the probability distribution (2.11) for particle transport perpendicular to the mean magnetic field is given by

$$\tilde{P}_{p\perp}(\tilde{x}, \tilde{y}, t|x_0, y_0, t_0) = \frac{1}{4\pi\kappa_{\perp}\Delta t} \exp\left(-\frac{(\tilde{x} + x_0 - x_1)^2 + (\tilde{y} + y_0 - y_1)^2}{4\kappa_{\perp}\Delta t}\right), \quad (2.16)$$

where $\tilde{P}_{p\perp}(\tilde{x}, \tilde{y}, t|x_0, y_0, t_0) \equiv P_{p\perp}(x, y, t|x_0, y_0, t_0)$. The analysis below shows that the probability distribution for particle transport across the field, P_{\perp} , can be expressed in terms of \tilde{r} and Δt and is independent of the azimuthal angle position coordinate ϕ .

It is also useful to consider the characteristic function

$$\hat{P}_{\perp}(k_1, k_2, t) = \int_{-\infty}^{\infty} d\tilde{x} \int_{-\infty}^{\infty} d\tilde{y} \exp[i(k_1\tilde{x} + k_2\tilde{y})] P_{\perp}(x, y, t|x_0, y_0, t_0). \quad (2.17)$$

The characteristic function $\hat{P}_{\perp}(k_1, k_2, t)$ can be used to calculate the moments of P_{\perp} of form $\langle \tilde{x}^m \tilde{y}^n \rangle$ in the usual way by evaluating the derivatives of the characteristic function $\partial^m \partial^n \hat{P}_{\perp} / \partial k_1^m \partial k_2^n$ at $\mathbf{k} = 0$.

Using (2.9), (2.10) and (2.16) for P_{FRW} , $P_{p\parallel}$ and $P_{p\perp}$ in (2.17) we obtain

$$\begin{aligned} \hat{P}_{\perp} = & \int_{-\infty}^{\infty} d\tilde{x} \int_{-\infty}^{\infty} d\tilde{y} \int_{-\infty}^{\infty} dx_1 \int_{-\infty}^{\infty} dy_1 \int_{-\infty}^{\infty} dz \frac{\exp[i(k_1\tilde{x} + k_2\tilde{y})]}{(4\pi D_L |\Delta z|)(4\pi\kappa_{\perp}\Delta t)(4\pi\kappa_{\parallel}\Delta t)^{1/2}} \\ & \times \exp\left(-\frac{(x_1 - x_0)^2 + (y_1 - y_0)^2}{4D_L |\Delta z|} - \frac{(\tilde{x} + x_0 - x_1)^2 + (\tilde{y} + y_0 - y_1)^2}{4\kappa_{\perp}\Delta t} \right. \\ & \left. - \frac{(\Delta z - V_z \Delta t)^2}{4\kappa_{\parallel}\Delta t}\right), \end{aligned} \quad (2.18)$$

where $\Delta z = z - z_0$ and $\Delta t = t - t_0$. Carrying out the integrals with respect to \tilde{x} and \tilde{y} in (2.18), we obtain

$$\begin{aligned} \hat{P}_{\perp} = & \int_{-\infty}^{\infty} dx_1 \int_{-\infty}^{\infty} dy_1 \int_{-\infty}^{\infty} dz \frac{\exp[-\kappa_{\perp} k_{\perp}^2 \Delta t + ik_1(x_1 - x_0) + ik_2(y_1 - y_0)]}{(4\pi D_L |\Delta z|)(4\pi\kappa_{\parallel}\Delta t)^{1/2}} \\ & \times \exp\left(-\frac{(x_1 - x_0)^2 + (y_1 - y_0)^2}{4D_L |\Delta z|} - \frac{(\Delta z - V_z \Delta t)^2}{4\kappa_{\parallel}\Delta t}\right), \end{aligned} \quad (2.19)$$

where $k_{\perp}^2 = k_1^2 + k_2^2$. Next carrying out the integrals with respect to x_1 and y_1 , we obtain the one-dimensional integral

$$\hat{P}_{\perp} = \int_{-\infty}^{\infty} d\Delta z \frac{1}{(4\pi\kappa_{\parallel}\Delta t)^{1/2}} \exp\left(-\kappa_{\perp} k_{\perp}^2 \Delta t - k_{\perp}^2 D_L |\Delta z| - \frac{(\Delta z - V_z \Delta t)^2}{4\kappa_{\parallel}\Delta t}\right), \quad (2.20)$$

for \hat{P}_{\perp} . The important point to note in (2.20) is that \hat{P}_{\perp} is a function of k_{\perp}^2 and Δt , and hence is azimuthally symmetric in \mathbf{k} -space.

By carrying out the integral over Δz in (2.20), \hat{P}_{\perp} can be expressed in terms of the complementary error function $\text{erfc}(z)$ in the form

$$\begin{aligned} \hat{P}_{\perp} = & \frac{1}{2} \exp\left(-\kappa_{\perp} k_{\perp}^2 \Delta t - \frac{V_z^2 \Delta t}{4\kappa_{\parallel}}\right) \\ & \times [\exp(\lambda_-^2 \Delta t) \text{erfc}(\lambda_- \sqrt{\Delta t}) + \exp(\lambda_+^2 \Delta t) \text{erfc}(\lambda_+ \sqrt{\Delta t})], \end{aligned} \quad (2.21)$$

where

$$\lambda_{\pm} = k_{\perp}^2 D_L \kappa_{\parallel}^{1/2} \mp \frac{V_z}{2\kappa_{\parallel}^{1/2}}, \quad (2.22)$$

(see Abramowitz and Stegun (1965), chapter 7, p 395 for detailed properties of the complementary error function).

By using the Laplace transform

$$\int_0^{\infty} \exp(-pt) \exp(a^2 t) \operatorname{erfc}(at) dt = \frac{1}{\sqrt{p}(\sqrt{p} + a)}, \quad (2.23)$$

(Erdelyi *et al* (1954), vol 1, formula 7, p 234), the Laplace transform of (2.21) with respect to Δt is

$$\tilde{P}_{\perp}(s, k_{\perp}) = \frac{1}{2\sqrt{\sigma}} \left(\frac{1}{\sqrt{\sigma} + \lambda_{+}} + \frac{1}{\sqrt{\sigma} + \lambda_{-}} \right), \quad (2.24)$$

where

$$\sigma = s + k_{\perp}^2 \kappa_{\perp} + \frac{V_z^2}{4\kappa_{\parallel}}. \quad (2.25)$$

The transform (2.24) gives the transform of P_{\perp} in the Fourier–Laplace space.

2.3. Asymptotics

The asymptotic evolution equation for $P_{\perp}(\tilde{\mathbf{x}}_{\perp}, t)$ at large space and time scales can be determined from the behavior of $\tilde{P}(k_{\perp}, s)$ as $s \rightarrow 0$ and as $k_{\perp} \rightarrow 0$. Similarly, the evolution equation for $P_{\perp}(\tilde{\mathbf{x}}_{\perp}, t)$ at early time and short space scales is associated with the behavior of $\tilde{P}(k_{\perp}, s)$ as $s \rightarrow \infty$ and $k_{\perp} \rightarrow \infty$. We first note from (2.24) and (2.25) that

$$\Phi(k_{\perp}, s) \tilde{P}_{\perp}(k_{\perp}, s) = 1, \quad (2.26)$$

where

$$\Phi(k_{\perp}, s) = \frac{\sqrt{\sigma}(\sqrt{\sigma} + \lambda_{+})(\sqrt{\sigma} + \lambda_{-})}{\sqrt{\sigma} + \bar{\lambda}}, \quad (2.27)$$

$$\lambda_{\pm} = k_{\perp}^2 D_L \sqrt{\kappa_{\parallel}} \mp \sqrt{v_{\text{cd}}}, \quad \bar{\lambda} = k_{\perp}^2 D_L \sqrt{\kappa_{\parallel}}, \quad (2.28)$$

$$\sigma = s + k_{\perp}^2 \kappa_{\perp} + v_{\text{cd}}, \quad v_{\text{cd}} = \frac{V_z^2}{4\kappa_{\parallel}}. \quad (2.29)$$

Here $v_{\text{cd}} \equiv 1/\tau_{\text{cd}} = V_z^2/(4\kappa_{\parallel})$, τ_{cd} is the convection–drift–diffusion time scale parallel to the magnetic field \mathbf{B} and $\ell_{\text{cd}} = \kappa_{\parallel}/V_z$ is the corresponding length scale.

2.3.1. Late time and long space scale expansion. Lowest order balance of terms for small s and k_{\perp}^2 with $s \sim k_{\perp}^2$ in (2.26) gives

$$\Phi = s + k_{\perp}^2 \kappa_{\perp} + \kappa_F k_{\perp}^2 - \frac{\kappa_F^2}{4v_{\text{cd}}} k_{\perp}^4 + O(s^3), \quad \kappa_F = |V_z| D_L. \quad (2.30)$$

Here, $\kappa_F = |V_z| D_L$ is the perpendicular diffusion due to field line random walk and the bulk advective transport of particles parallel to \mathbf{B} .

Using the usual Laplace–Fourier transform associations

$$s \rightarrow \partial_t, \quad \mathbf{k} \rightarrow -i\nabla, \quad k_{\perp}^2 \rightarrow -\nabla_{\perp}^2, \quad (2.31)$$

(2.26) and (2.30) give the long wavelength and long time scale evolution equation:

$$[\partial_t - (\kappa_{\perp} + \kappa_F) \tilde{\nabla}_{\perp}^2 - \kappa_{\parallel} D_L^2 \tilde{\nabla}_{\perp}^4] P_{\perp}(\tilde{\mathbf{x}}_{\perp}, t) = \delta(\tilde{\mathbf{x}}_{\perp}) \delta(t), \quad (2.32)$$

for $P_{\perp}(\tilde{\mathbf{x}}_{\perp}, t)$. Since $\tilde{\mathbf{x}}_{\perp} = \mathbf{x}_{\perp} - \mathbf{V}_{\perp} t$, (2.32) may be rewritten in the form

$$[\partial_t + \mathbf{V}_{\perp} \cdot \nabla_{\perp} - (\kappa_{\perp} + \kappa_F) \nabla_{\perp}^2 - \kappa_{\parallel} D_L^2 \nabla_{\perp}^4] P_{\perp}(\tilde{\mathbf{x}}_{\perp}, t) = \delta(\tilde{\mathbf{x}}_{\perp}) \delta(t). \quad (2.33)$$

Thus, at late times and long length scales, the cross-field diffusion coefficient $\kappa_{\perp}^{\text{eff}} = \kappa_{\perp} + \kappa_F$ consists of the kinetic, (microscopic) perpendicular diffusion coefficient, plus the field line random walk diffusion coefficient $\kappa_F = |V_z| D_L$ due to bulk advection and drift parallel to \mathbf{B} . The higher order, fourth derivative term $-\kappa_{\parallel} D_L^2 \nabla_{\perp}^4$ represents the late time effects of compound diffusion.

2.3.2. *Early time, short space scale expansion.* $\Phi(k_{\perp}, s)$ in (2.27) may be rewritten in the form

$$\Phi(k_{\perp}, s) = \sigma \left(1 + \frac{\bar{\lambda}}{\sqrt{\sigma}} - \frac{\nu_{\text{cd}}}{\sqrt{\sigma}(\sqrt{\sigma} + \bar{\lambda})} \right). \quad (2.34)$$

At early times and short length scales, balance of the first two terms in large parentheses in (2.34) requires that s scale as $s \sim k_{\perp}^4$ as $s \rightarrow \infty$. Thus, as $s \rightarrow \infty$ and $k_{\perp} \rightarrow \infty$ we obtain

$$\Phi(k_{\perp}, s) = s [1 + D_L \kappa_{\parallel}^{1/2} s^{-1/2} k_{\perp}^2 + O(k_{\perp}^{-2})]. \quad (2.35)$$

Using (2.35) in (2.26) and inverting back to $(\tilde{\mathbf{x}}, t)$ space, we obtain

$$\partial_t [1 - D_L \kappa_{\parallel}^{1/2} (\partial_t)^{-1/2} \tilde{\nabla}_{\perp}^2] P_{\perp}(\tilde{\mathbf{x}}_{\perp}, t) = \delta(\tilde{\mathbf{x}}_{\perp}) \delta(t), \quad (2.36)$$

as the evolution equation for $P_{\perp}(\tilde{\mathbf{x}}_{\perp}, t)$. Equation (2.36) is the fractional Fokker–Planck equation for compound diffusion (Sokolov *et al* (2002), Webb *et al* (2006), see also below for further discussion).

In the following subsection, we use (2.24) to formulate the Chapman–Kolmogorov equation (2.8) as a fractional Fokker–Planck equation.

2.4. Fractional Fokker–Planck equations

By using the Laplace–Fourier transform associations (2.31), the Laplace transform equation (2.25) for \tilde{P}_{\perp} can be inverted to yield a fractional diffusion equation for P_{\perp} in the form

$$L [L - \sqrt{\nu_{\text{cd}}} - D_L \sqrt{\kappa_{\parallel}} \nabla_{\perp}^2] [L + \sqrt{\nu_{\text{cd}}} - D_L \sqrt{\kappa_{\parallel}} \nabla_{\perp}^2] \times \{L - D_L \sqrt{\kappa_{\parallel}} \nabla_{\perp}^2\}^{-1} P_{\perp} = \delta(\mathbf{x}_{\perp}) \delta(t), \quad (2.37)$$

where $\nu_{\text{cd}} = V_z^2 / (4\kappa_{\parallel})$ is given by (2.29), and the pseudo-differential operator L is defined by

$$L = (\partial_t - \kappa_{\perp} \nabla_{\perp}^2 + \nu_{\text{cd}})^{1/2} \quad \text{and} \quad L^2 = \partial_t - \kappa_{\perp} \nabla_{\perp}^2 + \nu_{\text{cd}}. \quad (2.38)$$

The Case $V_z = 0$. In the special case $V_z = 0$, (2.37) simplifies to the equation

$$(\partial_t - \kappa_{\perp} \nabla_{\perp}^2) [1 - D_L \sqrt{\kappa_{\parallel}} (\partial_t - \kappa_{\perp} \nabla_{\perp}^2)^{-1/2} \nabla_{\perp}^2] P_{\perp} = \delta(\mathbf{x}_{\perp}) \delta(t). \quad (2.39)$$

In the limit as $\kappa_{\perp} \rightarrow 0$, (2.39) reduces to the standard compound diffusion equation

$$\partial_t [P_{\perp} - D_L \sqrt{\kappa_{\parallel}} \partial_t^{-1/2} \nabla_{\perp}^2 P_{\perp}] = \delta(\mathbf{x}_{\perp}) \delta(t), \quad (2.40)$$

where

$$\partial_t^{-\beta} f(t) = \frac{1}{\Gamma(\beta)} \int_0^t (t - t')^{\beta-1} f(t') dt' \quad (2.41)$$

is the Riemann–Liouville fractional integral (e.g., Erdelyi *et al* (1954), vol 2, p 181, Sokolov *et al* (2002)). Thus, in (2.40),

$$\partial_t^{-1/2} f(t) = \frac{1}{\sqrt{\pi}} \int_0^t (t-t')^{-1/2} f(t') dt', \quad (2.42)$$

and $\partial_t^{-1} f(t) = \int_0^t f(t') dt'$. The half-time derivative operator $\partial_t^{1/2}$ is defined by the equation $\partial_t^{1/2} = \partial_t \partial_t^{-1/2}$. Using (2.39)–(2.42) we obtain

$$\frac{\partial P_{\perp}}{\partial t} - D_L \sqrt{\kappa_{\parallel}} \partial_t \left\{ \frac{1}{\sqrt{\pi}} \int_0^t (t-t')^{-1/2} \nabla_{\perp}^2 P_{\perp}(\mathbf{x}, t') dt' \right\} = \delta(\mathbf{x}_{\perp}) \delta(t), \quad (2.43)$$

which is the fractional diffusion equation obtained by Webb *et al* (2006) to describe compound diffusion of cosmic rays in the case where the particles only diffuse parallel to the random walking magnetic field. The integral term in curly brackets in (2.43) is $\partial_t^{-1/2} \nabla_{\perp}^2 P_{\perp}$.

In the more general case where $\kappa_{\perp} \neq 0$ and $V_z = 0$, use of the Laplace–Fourier correspondence (2.31) gives

$$\begin{aligned} & -(\partial_t - \kappa_{\perp} \nabla_{\perp}^2)^{-1/2} \nabla_{\perp}^2 P_{\perp}(x, y, t) \\ &= \int_{-\infty}^{\infty} \frac{d^2 k}{4\pi^2} \int_{c-i\infty}^{c+i\infty} \frac{ds}{2\pi i} \frac{\exp[st - i(k_1 x + k_2 y)]}{\sqrt{s + k_{\perp}^2 \kappa_{\perp}}} k_{\perp}^2 \tilde{P}_{\perp}(\mathbf{k}, s), \end{aligned} \quad (2.44)$$

for the integral-differential operator in (2.39). Using the convolution theorem for both the Fourier and Laplace transforms in (2.44) we obtain the integral representation

$$\begin{aligned} & (\partial_t - \kappa_{\perp} \nabla_{\perp}^2)^{-1/2} \nabla_{\perp}^2 P_{\perp}(x, y, t) \\ &= \int_0^t \frac{dt'}{\sqrt{\pi(t-t')}} \int_{-\infty}^{\infty} dx' \int_{-\infty}^{\infty} dy' G(x, y, t|x', y', t') \nabla_{\perp}^2 P_{\perp}(x', y', t'), \end{aligned} \quad (2.45)$$

where

$$G(x, y, t|x', y', t') = \frac{1}{4\pi\kappa_{\perp}(t-t')} \exp\left(-\frac{(x-x')^2 + (y-y')^2}{4\kappa_{\perp}(t-t')}\right) H(t-t') \quad (2.46)$$

is the 2D Green’s function of the heat equation $(\partial_t - \kappa_{\perp} \nabla_{\perp}^2)\psi = 0$, and $H(t-t')$ is the Heaviside step function.

Comment 1. In the limit as $\kappa_{\perp} t \rightarrow 0$, the Green’s function G in (2.46) tends to the product of two Dirac delta functions, i.e., $G \rightarrow \delta(x-x')\delta(y-y')$ and the pseudo-differential operator $(\partial_t - \kappa_{\perp} \nabla_{\perp}^2)^{-1/2} \rightarrow \partial_t^{-1/2}$, and we recover compound diffusion equation (2.40) considered by Webb *et al* (2006).

Comment 2. The Green’s function G for the case $\kappa_{\perp} \neq 0$ consists of a Gaussian pulse, which can be thought of as a broadened delta function pulse. For the $\kappa_{\perp} = 0$ case considered by Webb *et al* (2006) (see also Sokolov *et al* (2002)), the pdf P_{\perp} for compound diffusion has a cusp at $x = 0$. The effect of a finite nonzero κ_{\perp} on this pdf will be to smooth out the distribution so that there is no cusp in P_{\perp} at $x = 0$.

Comment 3. Since $P_{\perp}(x, y, t)$ is cylindrically symmetric (i.e., only depends on $r = \sqrt{x^2 + y^2}$ and t), use of cylindrical coordinates r and θ in (2.45) gives

$$(\partial_t - \kappa_{\perp} \nabla_{\perp}^2)^{-1/2} \nabla_{\perp}^2 P_{\perp}(r, t) = \int_0^t \frac{dt'}{\sqrt{\pi(t-t')}} \int_0^{\infty} dr' r' \Gamma(r, t|r', t') \nabla_{\perp}^2 P_{\perp}(r', t'), \quad (2.47)$$

where $\nabla_{\perp}^2 P_{\perp} \equiv (1/r)\partial_r(r\partial_r P_{\perp})$ and

$$\Gamma(r, t|r', t') = \frac{1}{2\kappa_{\perp}(t-t')} \exp\left(-\frac{r^2+r'^2}{4\kappa_{\perp}(t-t')}\right) I_0\left(\frac{rr'}{2\kappa_{\perp}(t-t')}\right) H(t-t') \quad (2.48)$$

is the Green's function of the cylindrically symmetric heat equation:

$$\frac{\partial \Gamma}{\partial t} - \frac{\kappa_{\perp}}{r} \frac{\partial}{\partial r} \left(r \frac{\partial \Gamma}{\partial r} \right) = \frac{\delta(r-r')\delta(t-t')}{r'}, \quad (2.49)$$

and $I_0(z)$ is the modified Bessel function of the first kind of order zero. The result (2.47) can be obtained by converting the integrals over (x', y') in (2.45) to integrals over r' and θ' where $x' = r' \cos \theta'$ and $y' = r' \sin \theta'$, and by using the generating function identity

$$\exp(z \cos \theta) = I_0(z) + 2 \sum_{n=1}^{\infty} I_n(z) \cos(n\theta), \quad (2.50)$$

where $I_n(z)$ is the modified Bessel function of the first kind of order n (Abramowitz and Stegun (1965), formula 9.6.34, p 376).

The general case $\kappa_{\perp}, \kappa_{\parallel}, D_L$ and V_z all nonzero. In the general case where $\kappa_{\perp}, \kappa_{\parallel}, V_z$ and D_L are all nonzero, the Laplace–Fourier inversion of (2.26) gives the integral-differential evolution equation

$$(\partial_t - \kappa_{\perp} \nabla_{\perp}^2 + v_{cd}) \{P_{\perp}(\tilde{r}, t) - D_L \sqrt{\kappa_{\parallel}} \mathcal{I}_1 [P_{\perp}(\tilde{r}, t)] - v_{cd} \mathcal{I}_2 [P_{\perp}(\tilde{r}, t)]\} = \delta(\tilde{\mathbf{x}}_{\perp}) \delta(t), \quad (2.51)$$

where

$$-D_L \sqrt{\kappa_{\parallel}} \mathcal{I}_1 [P_{\perp}(\tilde{r}, t)] = \mathcal{L}^{-1} \left(\frac{\bar{\lambda}}{\sqrt{\sigma}} \tilde{P}_{\perp}(k_{\perp}, s) \right), \quad (2.52)$$

$$\mathcal{I}_2 [P_{\perp}(\tilde{r}, t)] = \mathcal{L}^{-1} \left(\frac{\tilde{P}_{\perp}(k_{\perp}, s)}{\sqrt{\sigma}(\sqrt{\sigma} + \bar{\lambda})} \right) \quad (2.53)$$

denote the inverse Fourier–Laplace transforms associated with $\Phi(k_{\perp}, s)$ in (2.34). The term (2.52) is associated with compound diffusion and field line random walk. The last term on the left-hand side of (2.51) is due to advection and drift, since it is proportional to $v_{cd} = V_z^2/(4\kappa_{\parallel})$. It is zero if $V_z = 0$.

Using the convolution for Fourier–Laplace transforms in (2.52) we obtain

$$\begin{aligned} \mathcal{I}_1 [P_{\perp}(\tilde{r}, t)] &= \int_0^t dt' \frac{dt'}{\sqrt{\pi}(t-t')} \exp[-v_{cd}(t-t')] \\ &\times \int_0^{\infty} dr' r' \Gamma(\tilde{r}, t|r', t') \nabla_{\perp}^2 P_{\perp}(r', t'), \end{aligned} \quad (2.54)$$

where $\Gamma(\tilde{r}, t|r', t')$ is the Green's function of the cylindrically symmetric heat equation (2.48). Thus, \mathcal{I}_1 is the generalization of the non-local diffusion operator (2.45) for cases where $v_{cd} = V_z^2/(4\kappa_{\parallel}) \neq 0$.

A similar Fourier–Laplace inversion of (2.53) gives

$$\begin{aligned} \mathcal{I}_2 [P_{\perp}(\tilde{r}, t)] &= \int_0^t dt' \int_0^{\infty} dr' r' \int_0^{\infty} d\zeta \frac{\exp(-\zeta^2) \exp(-v_{cd} \Delta t)}{\sqrt{\pi} \Lambda(\zeta, \Delta t)} \\ &\times \exp\left(-\frac{\tilde{r}^2+r'^2}{4\Lambda(\zeta, \Delta t)}\right) I_0\left(\frac{\tilde{r}r'}{2\Lambda(\zeta, \Delta t)}\right) P_{\perp}(r', t'), \end{aligned} \quad (2.55)$$

where

$$\Lambda(\zeta, \Delta t) = \kappa_{\perp} \Delta t + 2\zeta D_L \sqrt{\kappa_{\parallel}} \sqrt{\Delta t}, \quad \Delta t = t - t'. \quad (2.56)$$

The presence of the $\exp(-\zeta^2)$ term in (2.55) indicates that the dominant contribution to the ζ integral will, in general come from near $\zeta \approx 0$. The parameter ζ in (2.56) controls the relative importance of regular cross-field diffusion represented by $\kappa_{\perp} \Delta t$ and that of compound diffusion represented by $2\zeta D_L \sqrt{\kappa_{\parallel}} \sqrt{\Delta t}$.

2.5. Hankel transform formulation

Using the standard formula for the inverse Fourier transform in (2.17) we obtain

$$P_{\perp} = \frac{1}{4\pi^2} \int_{-\infty}^{\infty} dk_1 \int_{-\infty}^{\infty} dk_2 \exp[-i(k_1 \tilde{x} + k_2 \tilde{y})] \hat{P}_{\perp}(k_1, k_2, t). \quad (2.57)$$

Since \hat{P}_{\perp} depends only on $k_{\perp} = (k_1^2 + k_2^2)^{1/2}$ and Δt , it is convenient to use cylindrical polar coordinates in \mathbf{k} -space, with polar axis along the k_3 - or k_z -direction, and with $(k_1, k_2) = k_{\perp}(\cos \Phi, \sin \Phi)$, and also to use polar coordinates in (\tilde{x}, \tilde{y}) -space, with $(\tilde{x}, \tilde{y}) = \tilde{r}(\cos \phi, \sin \phi)$ as in (2.15). Then noting that

$$k_1 \tilde{x} + k_2 \tilde{y} = k_{\perp} \tilde{r} \cos(\Phi - \phi) \quad (2.58)$$

and using the generating function identity for Bessel functions (Abramowitz and Stegun (1965), formula 9.1.41, p 361), it follows that

$$\exp(-i\mathbf{k} \cdot \tilde{\mathbf{r}}) = \sum_{n=-\infty}^{\infty} \exp\left[-in\left(\frac{\pi}{2} + \phi - \Phi\right)\right] J_n(k_{\perp} \tilde{r}). \quad (2.59)$$

Then converting to polar coordinates in \mathbf{k} -space in (2.57), noting that $dk_1 dk_2 = k_{\perp} dk_{\perp} d\Phi$ and carrying out the integration over the azimuthal angle Φ , we obtain

$$P_{\perp} = \frac{1}{2\pi} \int_0^{\infty} dk_{\perp} k_{\perp} J_0(k_{\perp} \tilde{r}) \hat{P}(k_{\perp}, t). \quad (2.60)$$

The integrals over Φ for the separate Bessel function terms in the series for $n \neq 0$ vanish identically because of the periodicity of the $\exp(-in\Phi)$ terms in (2.59). Equation (2.60) shows that P_{\perp} depends only on \tilde{r} and t .

Similarly, using polar coordinates \tilde{r} and ϕ , and (2.58) and (2.59) in (2.17) we obtain

$$\hat{P}_{\perp}(k_{\perp}, t) = 2\pi \int_0^{\infty} d\tilde{r} \tilde{r} J_0(k_{\perp} \tilde{r}) P_{\perp}(\tilde{r}, t), \quad (2.61)$$

where in an abuse of mathematical notation, we use $P_{\perp}(\tilde{r}, t)$ and $\hat{P}_{\perp}(k_{\perp}, t)$ to denote $P_{\perp}(\tilde{x}, \tilde{y}, t | x_0, y_0, t_0)$ and $\hat{P}_{\perp}(k_1, k_2, t)$, respectively.

Equations (2.60) and (2.61) show that $\hat{P}(k_{\perp}, t)$ and $P_{\perp}(\tilde{r}, t)$ form a Hankel transform pair (e.g., Erdelyi *et al* (1954), vol 2, p 3; note that the normalization used in our definition is different than that used by Erdelyi *et al* (1954)). From (2.20) or (2.21) it follows that $\hat{P}_{\perp}(0, t) = 1$. Using this result in (2.57) shows that the double integral of P_{\perp} over the whole (\tilde{x}, \tilde{y}) plane is equal to 1, and hence P_{\perp} is a properly normalized probability distribution.

Using the expression (2.20) for \hat{P}_{\perp} in (2.60) we obtain

$$P_{\perp} = \int_{-\infty}^{\infty} \frac{d\Delta z}{(4\pi\kappa_{\parallel}\Delta t)^{1/2}} \exp\left(-\frac{(\Delta z - V_z \Delta t)^2}{4\kappa_{\parallel}\Delta t}\right) \times \frac{1}{2\pi} \int_0^{\infty} dk_{\perp} k_{\perp} J_0(k_{\perp} \tilde{r}) \exp[-k_{\perp}^2(\kappa_{\perp} \Delta t + D_L |\Delta z|)]. \quad (2.62)$$

Then carrying out the k_{\perp} integral using the Laplace transform:

$$\int_0^{\infty} \exp(-pt) J_0(2\alpha^{1/2}t^{1/2}) dt = \frac{1}{p} \exp\left(-\frac{\alpha}{p}\right), \quad (2.63)$$

(Erdelyi *et al* (1954), vol 1, formula 25, p 185) with the replacements $t \rightarrow k_{\perp}^2$, $p \rightarrow \kappa_{\perp}\Delta t + D_L|\Delta z|$, $\alpha \rightarrow \tilde{r}^2/4$, we obtain

$$P_{\perp} = \int_{-\infty}^{\infty} \frac{d\Delta z}{(4\pi\kappa_{\parallel}\Delta t)^{1/2}} \frac{1}{4\pi(\kappa_{\perp}\Delta t + D_L|\Delta z|)} \times \exp\left(-\frac{(\Delta z - V_z\Delta t)^2}{4\kappa_{\parallel}\Delta t} - \frac{\tilde{r}^2}{4(\kappa_{\perp}\Delta t + D_L|\Delta z|)}\right). \quad (2.64)$$

Hence, the probability distribution $P_{\perp}(\tilde{r}, t)$ can be determined by evaluating the integral (2.64).

Equation (2.64) for P_{\perp} is one of the main results for the paper. It can be used to determine the moments of P_{\perp} (section 2.6 and appendix A). If $D_L = 0$, use of (2.64) gives the heat equation Green's function for cross-field diffusion due to κ_{\perp} . The compound diffusion case for cylindrical symmetry about the z -axis (the mean field direction) is recovered if $V_z = \kappa_{\perp} = 0$ (section 3). The integral form (2.64) is also important for the numerical evaluation of P_{\perp} (section 3).

2.6. Moments

The n th order moment of \tilde{r} is defined as

$$\langle \tilde{r}^n \rangle = \int_{-\infty}^{\infty} dx \int_{-\infty}^{\infty} dy P_{\perp}(\tilde{x}, \tilde{y}, t) \tilde{r}^n \equiv 2\pi \int_0^{\infty} d\tilde{r} \tilde{r}^{n+1} P_{\perp}(\tilde{r}, t). \quad (2.65)$$

Other moments such as $\langle \tilde{x}^m \tilde{y}^n \rangle$ are defined in a similar fashion. In particular, one finds that all odd order moments of form $\langle \tilde{x}^m \tilde{y}^n \rangle$ where $m + n = 2N + 1$ are zero (e.g., $\langle \tilde{x}^3 \rangle = \langle \tilde{r}^3 \rangle \langle \cos^3 \phi \rangle = 0$). Note that the odd moments $\langle \tilde{r}^{2n+1} \rangle$ are nonzero. For the second-order moments:

$$\langle \tilde{x}^2 \rangle = \langle \tilde{y}^2 \rangle = \frac{1}{2} \langle \tilde{r}^2 \rangle, \quad \langle \tilde{x} \tilde{y} \rangle = 0. \quad (2.66)$$

The third-order moments of form $\langle \tilde{x}^m \tilde{y}^n \rangle$ with $m + n = 3$ are all zero, but $\langle \tilde{r}^3 \rangle \neq 0$. For the fourth-order moments:

$$\langle \tilde{x}^4 \rangle = \langle \tilde{y}^4 \rangle = \frac{3}{8} \langle \tilde{r}^4 \rangle, \quad \langle \tilde{x}^2 \tilde{y}^2 \rangle = \frac{1}{8} \langle \tilde{r}^4 \rangle. \quad (2.67)$$

By using the Taylor series expansion for $J_0(k_{\perp}\tilde{r})$ in (2.61) and equating powers of k_{\perp}^{2n} it follows that

$$\langle \tilde{r}^{2n} \rangle = (-1)^n 4^n n! \left(\frac{d^n \hat{P}_{\perp}}{d(k_{\perp}^2)^n} \right)_0, \quad (2.68)$$

This formula can be used to calculate the even moments of \tilde{r} , but it cannot be used to determine the odd moments $\langle \tilde{r}^{2n+1} \rangle$.

A method for calculating the moments $\langle \tilde{r}^n \rangle$ for both odd and even n is described in appendix A. From (A.11) we obtain

$$\langle \tilde{x}^2 \rangle = 2\kappa_{\perp}t + 2D_L V_z t \operatorname{erf}\left(\frac{V_z t^{1/2}}{2\kappa_{\parallel}^{1/2}}\right) + 4 \left(\frac{\kappa_{\parallel} D_L^2 t}{\pi}\right)^{1/2} \exp\left(-\frac{V_z^2 t}{4\kappa_{\parallel}}\right), \quad (2.69)$$

for the nonzero, second-order moment $\langle \tilde{x}^2 \rangle$ (note that $\langle \tilde{y}^2 \rangle = \langle \tilde{x}^2 \rangle$ and $\langle \tilde{r}^2 \rangle = 2\langle \tilde{x}^2 \rangle$). Without loss of generality, we have set $t_0 = 0$ in (2.69) so that $\Delta t \rightarrow t$. This convention will be applied to all formulae in the following analysis. Formulae (2.69) show the mutual interaction

of microscopic cross-field diffusion (κ_{\perp}), parallel diffusion (κ_{\parallel}), field line random walk (D_L) and drift/advection (V_z) on the cross-field particle transport across the random walking magnetic field.

Using the power series expansion of the exponential function and the error function for small arguments (Abramowitz and Stegun (1965, formula 7.1.5, p 297)) in (2.69), we find

$$\begin{aligned} \langle \tilde{x}^2 \rangle = \langle \tilde{y}^2 \rangle &\approx 2\kappa_{\perp}t + \frac{D_L V_z^2}{(\pi\kappa_{\parallel})^{1/2}} t^{3/2} + 4 \left(\frac{\kappa_{\parallel} D_L^2}{\pi} \right)^{1/2} t^{1/2} \\ &\approx 4 \left(\frac{\kappa_{\parallel} D_L^2}{\pi} \right)^{1/2} t^{1/2}, \end{aligned} \quad (2.70)$$

in the limit of small t . Thus, at early times, the particle propagation across the field in this model is subdiffusive and behaves according to the compound diffusion model (e.g., Kota and Jokipii (2000), Webb *et al* (2006)), in which particles are confined to move diffusively along the random walking magnetic field line. However, if one uses the telegrapher equation model, in which there is ballistic particle transport along the magnetic field at early times, with no cross-field diffusion ($\kappa_{\perp} = 0$) and drift, then the particle transport across the field is diffusive due to the combined effects of random walking field lines and ballistic transport with $\langle (\Delta x)^2 \rangle \sim v D_L t$ (Webb *et al* (2006)).

Using the asymptotic expansion for $\text{erfc}(z) = 1 - \text{erf}(z)$ for large $|z|$ (Abramowitz and Stegun (1965), formula 7.1.23, p 298) in (2.69), we obtain

$$\begin{aligned} \langle \tilde{x}^2 \rangle = \langle \tilde{y}^2 \rangle &\approx 2(\kappa_{\perp} + V_z D_L)t + 8 \left(\frac{\kappa_{\parallel} D_L^2}{\pi t} \right)^{1/2} \frac{\kappa_{\parallel}}{V_z^2} \exp\left(-\frac{V_z^2 t}{4\kappa_{\parallel}}\right) \\ &\approx 2(\kappa_{\perp} + V_z D_L)t, \end{aligned} \quad (2.71)$$

in the limit as $t \rightarrow \infty$. Hence at late times, (2.71) shows that the particle transport across the field is diffusive with an effective diffusion coefficient

$$\kappa_{\perp e} = \frac{\langle \tilde{x}^2 \rangle}{2t} = \frac{\langle \tilde{y}^2 \rangle}{2t} = \kappa_{\perp} + V_z D_L. \quad (2.72)$$

The result (2.72) shows that the effective cross-field diffusion coefficient at late times consists of the microscopic perpendicular diffusion coefficient κ_{\perp} plus a field line random walk contribution $\kappa_{\perp}^{\text{FRW}} = V_z D_L$ (see also Webb *et al* (2008), Shalchi *et al* (2009a)).

The effective running diffusion coefficient for cross-field transport $\kappa_{\perp e} = \langle \tilde{x}^2 \rangle / (2t)$ is given by

$$\kappa_{\perp e} = \kappa_{\perp} + D_L V_z \text{erf}\left(\frac{V_z t^{1/2}}{2\kappa_{\parallel}^{1/2}}\right) + 2 \left(\frac{\kappa_{\parallel} D_L^2}{\pi t} \right)^{1/2} \exp\left(-\frac{V_z^2 t}{4\kappa_{\parallel}}\right). \quad (2.73)$$

One can show that $\kappa_{\perp e}(t)$ is a monotonic decreasing function of t , with $\kappa_{\perp e} \sim 2\sqrt{\kappa_{\parallel}/\pi} D_L t^{-1/2}$ at small t (i.e., subdiffusion at small t), and with $\kappa_{\perp e} \rightarrow \kappa_{\perp} + V_z D_L$ as $t \rightarrow \infty$. Note that the classical compound diffusion term in (2.69), (the last term on the right-hand side) is strongly damped at late times if $V_z \neq 0$. However, if $V_z = 0$, then it scales like $t^{1/2}$ and is not damped exponentially at late times.

The effective cross-field diffusion coefficient in (2.73) can be written in the dimensionless form

$$\bar{\kappa}_{\perp e} = \alpha + \beta \left[\text{erf}\left(\frac{1}{2}\sqrt{\bar{t}}\right) + \frac{2}{\sqrt{\pi\bar{t}}} \exp\left(-\frac{\bar{t}}{4}\right) \right], \quad (2.74)$$

where $\bar{\kappa}_{\perp e}(\bar{t}) = \kappa_{\perp e} / \kappa_{\parallel}$. Here $\bar{t} = V_z^2 t / \kappa_{\parallel}$ and $\bar{x} = V_z x / \kappa_{\parallel}$ are dimensionless time and space coordinates, based on the advection–diffusion time and length scales. The parameters

$$\alpha = \frac{\kappa_{\perp}}{\kappa_{\parallel}}, \quad \beta = \frac{|V_z| D_L}{\kappa_{\parallel}} = \frac{\kappa_F}{\kappa_{\parallel}}, \quad \kappa_F = |V_z| D_L \quad (2.75)$$

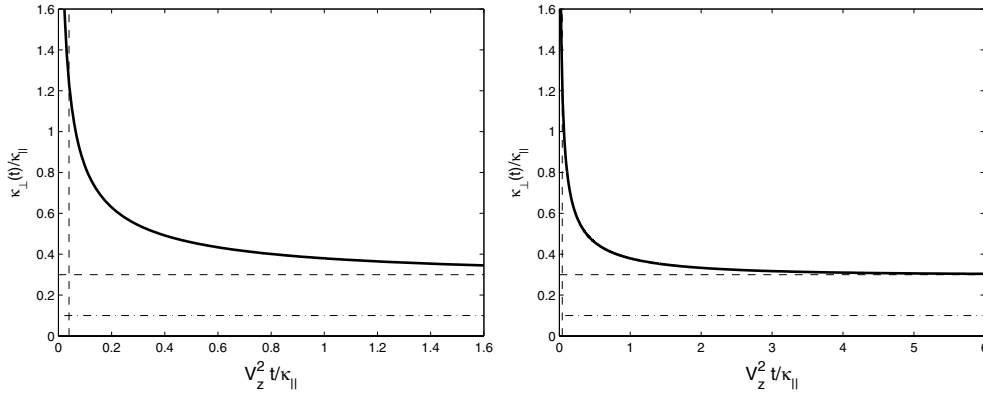


Figure 1. shows the effective perpendicular diffusion coefficient $\bar{\kappa}_{\perp e}(\bar{t})$ of (3.15) versus \bar{t} for the case $\alpha = 0.1$ and $\beta = 0.2$ where $\bar{t} = t/T_2$ and $T_2 = \kappa_{\parallel}/V_z^2$ is the advection–diffusion time scale. In the left panel $0 < \bar{t} < 1.6$, but $0 < \bar{t} < 6$ for the right panel.

describe the effects of local cross-field diffusion (α) and cross-field diffusion due to field line random walk (β).

Figure 1 shows a plot of $\bar{\kappa}_{\perp e}$ versus \bar{t} for the case $\alpha = 0.1$ and $\beta = 0.2$. The running diffusion coefficient $\bar{\kappa}_{\perp e}$ is a monotonic decreasing function of \bar{t} , with $\bar{\kappa}_{\perp e} \propto \bar{t}^{-1/2}$ at small \bar{t} , during the compound diffusion phase, and $\bar{\kappa}_{\perp e} \rightarrow \alpha + \beta$ as $\bar{t} \rightarrow \infty$ in the late time diffusion phase. The horizontal dashed line corresponds to the value of the perpendicular diffusion coefficient obtained in the absence of field line random walk. The compound diffusion phase is delimited by the requirement that the particle must have undergone many scatters along the field line. This requires that $t \gg T_1 = D_L^2/\kappa_{\parallel}$ or $\bar{t} \gg \beta^2$. The vertical dashed line corresponds to the condition $\bar{t} = \beta^2$. For $\bar{t} < \beta^2$ other physical effects not included in the model come into play (e.g., non-diffusive particle transport, ballistic or telegrapher equation effects and field line decorrelation effects due to the magnetic field stochastic instability (e.g., Rechester and Rosenbluth *et al* (1978))).

The higher order moments are useful in elucidating different physical effects. For example, one can show that

$$\langle \tilde{x}^4 \rangle = \langle \tilde{y}^4 \rangle = 12C_2, \quad \langle \tilde{x}^2 \tilde{y}^2 \rangle = 4C_2, \quad \langle \tilde{r}^4 \rangle = 32C_2, \quad (2.76)$$

where C_2 and the associated integrals \mathcal{I}_4^{\pm} are defined in appendix A. We obtain the formulae

$$C_2 = \mathcal{I}_4^- + \mathcal{I}_4^+ \equiv (d^2 \hat{P}_{\perp} / d(k_{\perp}^2))^0. \quad (2.77)$$

Evaluation of (2.77) gives

$$C_2 = \left[\kappa_{\perp}^2 + (V_z D_L)^2 + 2\kappa_{\perp} V_z D_L \operatorname{erf} \left(\frac{V_z t^{1/2}}{2\kappa_{\parallel}^{1/2}} \right) \right] t^2 + 2\kappa_{\parallel} D_L^2 t + 2\kappa_{\perp} t \left(\frac{4\kappa_{\parallel} D_L^2 t}{\pi} \right)^{1/2} \exp \left(-\frac{V_z^2 t}{4\kappa_{\parallel}} \right). \quad (2.78)$$

Note that the compound diffusion term $2\kappa_{\parallel} D_L^2 t$ in (2.78) is not exponentially damped and persists at large times. In fact at late times $t \rightarrow \infty$,

$$C_2 \approx (\kappa_{\perp} + V_z D_L)^2 t^2 + 2\kappa_{\parallel} D_L^2 t, \quad (2.79)$$

$$\langle \tilde{x}^4 \rangle = \langle \tilde{y}^4 \rangle \approx 12 [(\kappa_{\perp} + V_z D_L)^2 t^2 + 2\kappa_{\parallel} D_L^2 t].$$

Hence, at late times, the behavior of the moments (2.79) indicates that at the lowest order the transport across the field is normal diffusion with diffusion coefficient (2.72). However, there is a higher order contribution at intermediate times from compound diffusion (the t term in (2.79)). At early times ($t \rightarrow 0$),

$$C_2 \approx 2\kappa_{\parallel} D_L^2 t, \quad \langle \tilde{x}^4 \rangle = \langle \tilde{y}^4 \rangle \approx 24\kappa_{\parallel} D_L^2 t, \quad (2.80)$$

which indicates that compound diffusive behavior (i.e., subdiffusive behavior) is obtained at early times.

3. Solution examples

We first note that the solution (2.64) for P_{\perp} can be reduced to the dimensionless form by the introduction of dimensionless space and time variables:

$$\bar{\mathbf{x}} = \frac{\mathbf{x}}{L}, \quad \bar{t} = \frac{t}{T}, \quad (3.1)$$

where L and T are characteristic length and time scales. Without loss of generality, we replace $\Delta \mathbf{x}$ by \mathbf{x} and Δt by t , in the following analysis (i.e., we set $\mathbf{x}_0 = 0$ and $t_0 = 0$). Using the variables (3.1), the solution (2.64) for P_{\perp} can be written in the dimensionless form

$$p_{\perp} = P_{\perp} L^2 = \int_{-\infty}^{\infty} \frac{d\theta}{\sqrt{\pi}} \frac{\exp[-\theta^2 - \bar{r}^2/(4\zeta)]}{4\pi\zeta}, \quad (3.2)$$

where

$$\zeta = \bar{\kappa}_{\perp} \bar{t} + \bar{D}_L |\bar{V}_z \bar{t} + 2(\bar{\kappa}_{\parallel} \bar{t})^{1/2} \theta|. \quad (3.3)$$

Here, $\bar{\kappa}_{\perp}$, $\bar{\kappa}_{\parallel}$, \bar{D}_L and \bar{V}_z are dimensionless versions of κ_{\perp} , κ_{\parallel} , D_L and V_z , namely,

$$\bar{\kappa}_{\perp} = \frac{\kappa_{\perp} T}{L^2}, \quad \bar{\kappa}_{\parallel} = \frac{\kappa_{\parallel} T}{L^2}, \quad \bar{D}_L = \frac{D_L}{L}, \quad \bar{V}_z = \frac{V_z T}{L}. \quad (3.4)$$

In general, the moments of P_{\perp} can be expressed in the dimensionless form. In particular, from (2.64) we obtain $\langle \bar{x}^2 \rangle = \langle \bar{y}^2 \rangle$ with

$$\langle \bar{x}^2 \rangle = 2\bar{\kappa}_{\perp} \bar{t} + 2(\bar{D}_L \bar{V}_z \bar{t}) \operatorname{erf} \left(\frac{\bar{V}_z \bar{t}^{1/2}}{2\bar{\kappa}_{\parallel}^{1/2}} \right) + 4 \left(\frac{\bar{\kappa}_{\parallel} \bar{D}_L^2 \bar{t}}{\pi} \right)^{1/2} \exp \left(-\frac{\bar{V}_z^2 \bar{t}}{4\bar{\kappa}_{\parallel}} \right), \quad (3.5)$$

as the dimensionless form of the variances $\langle \bar{x}^2 \rangle$ and $\langle \bar{y}^2 \rangle$ of P_{\perp} .

The main points to note about the solution (3.2)–(3.3) for p_{\perp} and the variance formulae (3.5) are that they depend on the four independent parameters $\bar{\kappa}_{\perp}$, $\bar{\kappa}_{\parallel}$, \bar{D}_L and \bar{V}_z listed in (3.4).

Before presenting numerical examples of the solutions for p_{\perp} and the variances, it is instructive to consider special cases of the solution for p_{\perp} . If we set $\bar{\kappa}_{\parallel} = 0$ in (3.2) and (3.3) we obtain the heat equation Green's function solution

$$p_{\perp} = \frac{1}{4\pi \bar{\kappa}_p \bar{t}} \exp \left(-\frac{\bar{r}^2}{4\bar{\kappa}_p \bar{t}} \right), \quad (3.6)$$

where $\bar{\kappa}_p = \bar{\kappa}_{\perp} + |\bar{V}_z| \bar{D}_L$ is the effective cross-field diffusion coefficient for the particles, due to local cross-field diffusion ($\bar{\kappa}_{\perp}$), and due to field line random walk ($\bar{\kappa}_F = |\bar{V}_z| \bar{D}_L$). In this mathematical limit, there is no parallel diffusion (this limit cannot be obtained physically, since $\kappa_{\perp} < \kappa_{\parallel}$ in standard quasilinear theory with no field line random walk, but it is possible that both κ_{\perp} and κ_{\parallel} are small), the particles undergo bulk advection along the magnetic field, with speed $|\bar{V}_z|$, and the particles diffuse perpendicular to the mean field. This situation is mathematically analogous to the case of ballistic transport of particles along the field, in which

the particle velocity v_z has been replaced by the bulk advection speed $|V_z|$, and the particles undergo cross-field diffusion due to field line random walk (e.g., Jokipii and Parker (1969)). Similarly, if we set $\bar{D}_L = 0$, there is no field line random walk, and the solution (3.2)–(3.3) for p_\perp again reduces to the heat equation Green’s function (3.6), except that now $\bar{\kappa}_p = \bar{\kappa}_\perp$ is due solely to local cross-field diffusion.

A further interesting limit of the solution (3.2)–(3.3) for p_\perp is obtained by setting $\bar{\kappa}_\perp = \bar{V}_z = 0$. In this limit, the solution for p_\perp reduces to

$$p_\perp = \int_{-\infty}^{\infty} \frac{d\theta}{\sqrt{\pi}} \frac{1}{8\pi \bar{D}_L (\bar{\kappa}_\parallel \bar{t})^{1/2} |\theta|} \exp\left(-\theta^2 - \frac{\bar{r}^2}{8\bar{D}_L (\bar{\kappa}_\parallel \bar{t})^{1/2} |\theta|}\right). \quad (3.7)$$

The solution (3.7) describes cross-field transport due to compound diffusion (e.g., Kota and Jokipii (2000), Webb *et al* (2006)). It is equivalent to the inverse Laplace transform solution for p_\perp given by Webb *et al* (2006) (equation (3.24)), in which there is cylindrical symmetry about the background magnetic field. In appendix B, we show that the solution can be expressed in terms of a Meijer G function (e.g., Erdelyi *et al* (1953) *Higher Transcendental Functions* vol 1, p 206, section 5.3). It was noted in Webb *et al* (2006) that $p_\perp \sim (C/\sqrt{\bar{t}}) \ln(r^2/\sqrt{\bar{t}})$ as $r \rightarrow 0$ for the compound diffusion solution (3.7), where C is a constant. Note that the solution (3.7) depends on the similarity variable $\bar{r}^2/\sqrt{\bar{t}}$ characteristic of compound diffusion. For the solution (3.7), the variance (3.5) reduces to

$$\langle \bar{x}^2 \rangle = \langle \bar{y}^2 \rangle = 4 \left(\frac{\bar{\kappa}_\parallel \bar{D}_L^2 \bar{t}}{\pi} \right)^{1/2}, \quad (3.8)$$

which is the variance for compound diffusion obtained by Kota and Jokipii (2000) and Webb *et al* (2006).

Two natural length and time scales in the system are

$$L_1 = D_L, \quad T_1 = \frac{D_L^2}{\kappa_\parallel}, \quad (3.9)$$

$$L_2 = \frac{\kappa_\parallel}{V_z}, \quad T_2 = \frac{\kappa_\parallel}{V_z^2}. \quad (3.10)$$

The length scale $L_1 = D_L$ is the random walk diffusion coefficient, for the magnetic field, and T_1 is the time for the particle to diffuse parallel to the magnetic field over the distance D_L . These length and time scales can only be used in cases where $D_L \neq 0$ (i.e., they do not apply if $D_L = 0$). The advection–diffusion length and time scales L_2 and T_2 are useful in describing the late time and long scale length behavior of P_\perp and the variances, but they only apply for cases where $V_z \neq 0$.

If one uses the length and time scales, $L_1 = D_L$ and $T_1 = D_L^2/\kappa_\parallel$, in the solution (3.2)–(3.3), then the four parameters (3.4) describing the solution are given by

$$\bar{\kappa}_\parallel = 1, \quad \bar{\kappa}_\perp = \alpha, \quad \bar{D}_L = 1, \quad |\bar{V}_z| = \beta, \quad L = L_1, \quad T = T_1, \quad (3.11)$$

where the parameters α and β are given by

$$\alpha = \frac{\kappa_\perp}{\kappa_\parallel}, \quad \beta = \frac{|V_z| D_L}{\kappa_\parallel} = \frac{\kappa_F}{\kappa_\parallel}, \quad \kappa_F = |V_z| D_L. \quad (3.12)$$

The parameters α and β describe the cross-field particle diffusion coefficients due to local perpendicular diffusion (κ_\perp) and due to field line random walk ($\kappa_F = |V_z| D_L$), respectively.

Similarly, if one uses the advection–diffusion length and time scales L_2 and T_2 in the solution (3.2)–(3.3) for p_\perp , then

$$\bar{\kappa}_\parallel = 1, \quad \bar{\kappa}_\perp = \alpha, \quad \bar{D}_L = \beta, \quad |\bar{V}_z| = 1, \quad L = L_2, \quad T = T_2. \quad (3.13)$$

In this case, $\bar{\kappa}_\parallel = |\bar{V}_z| = 1$ are fixed and $\bar{\kappa}_\perp = \alpha$, and $\bar{D}_L = \beta$ are arbitrary.

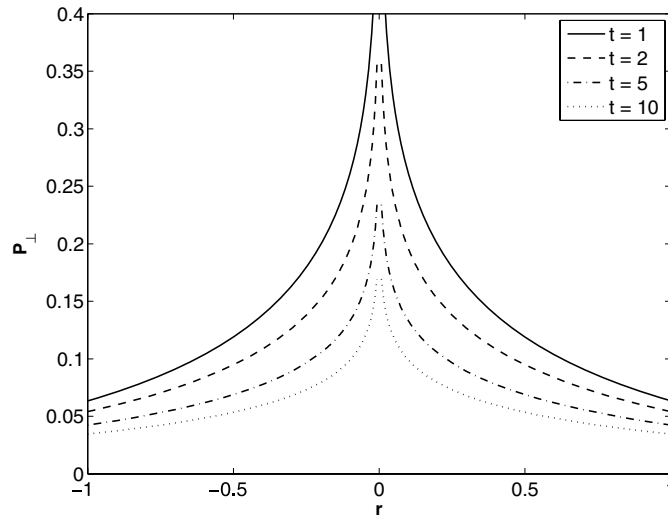


Figure 2. p_{\perp} versus \bar{r} for the case $\alpha = \beta = 0$, using the length and time scales $L_1 = D_L$ and $T_1 = D_L^2/\kappa_{\parallel}$ for a range of \bar{t} ($\bar{t} = 1, 2, 5, 10$). This corresponds to the compound diffusion solution (3.7) with cylindrical symmetry about the mean magnetic field with $\kappa_{\perp} = V_z = 0$ but $\kappa_{\parallel} \neq 0$ and $D_L \neq 0$. Note $p_{\perp} \rightarrow \infty$ as $\bar{r} \rightarrow 0$.

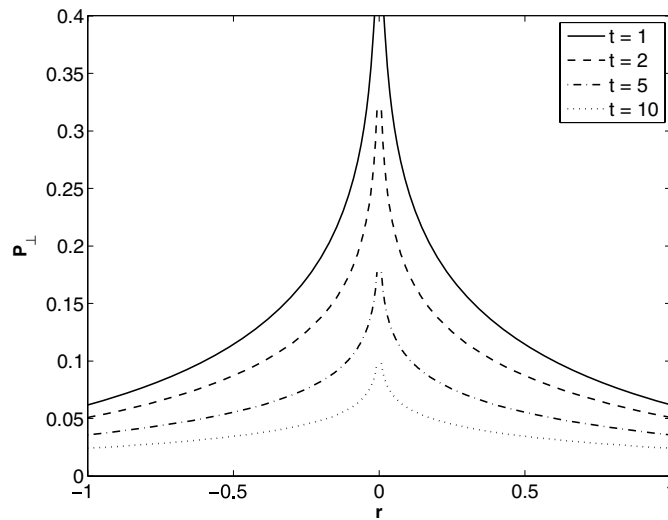


Figure 3. p_{\perp} versus \bar{r} for the case $\alpha = 0$ and $\beta = 0.5$ using the same length and time scales as figure 2, and for the same range of \bar{t} ($\bar{t} = 1, 2, 5, 10$). Because $\kappa_{\perp} = 0$, $p_{\perp} \rightarrow \infty$ as $r \rightarrow 0$. Note $V_z \neq 0$ and $D_L \neq 0$.

In figures 2–5, we use $L_1 = D_L$ and $T_1 = D_L^2/\kappa_{\parallel}$ as the length and time scales. Hence, $\bar{\kappa}_{\parallel} = \bar{D}_L = 1$, and $\bar{\kappa}_{\perp} = \alpha$ and $|\bar{V}_z| = \beta$ as in (3.11)–(3.12). Figure 2 shows the radial distribution of p_{\perp} in (3.7) for $\alpha = \beta = 0$ at times $\bar{t} = 1, 2, 5$ and 10. This solution corresponds to the case of classical compound diffusion, in which there is no local cross-field diffusion ($\kappa_{\perp} = 0$) and no advection or drift ($V_z = 0$). The particles are restricted to diffuse

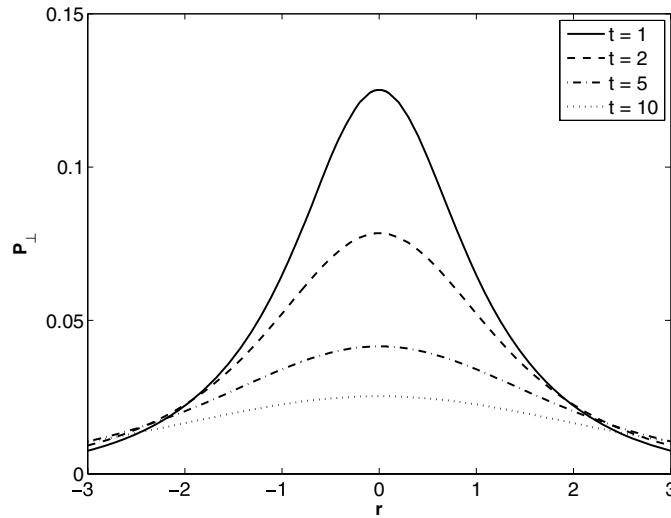


Figure 4. Same as figure 2 except $\alpha = 0.1$ and $\beta = 0$ (i.e., $V_z = 0$, $\kappa_{\perp} \neq 0$ and $D_L \neq 0$).

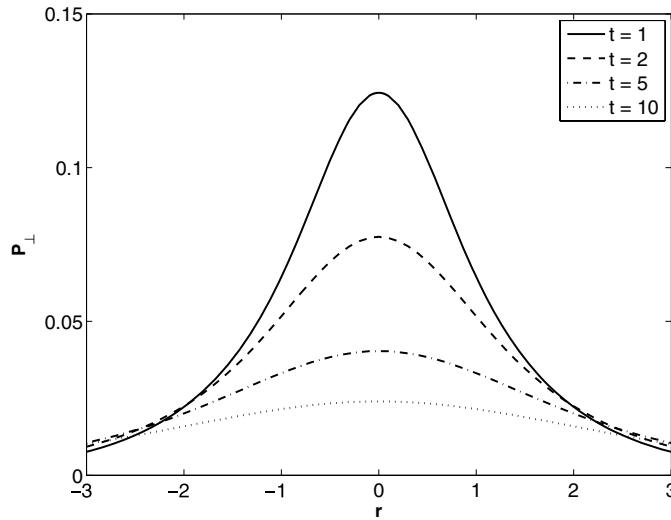


Figure 5. p_{\perp} versus \bar{r} for a range of \bar{t} ($\bar{t} = 1, 2, 5, 10$), for $\alpha = 0.1$ and $\beta = 0.2$ (cf figure 2).

along the random walking magnetic field. The net effect is subdiffusion of the particles across the mean field with $\langle \bar{r}^2 \rangle \propto \bar{t}^{1/2}$ as in (3.8) (see, e.g., the discussion by Kota and Jokipii (2000) and Webb *et al* (2006)). The profiles show a cusp in the distribution at $\bar{r} = 0$. Figure 3 shows how the profile of p_{\perp} in (3.2)–(3.3) changes if $\kappa_{\perp} = 0$ and $V_z \neq 0$ ($\alpha = 0$ and $\beta = 0.5$), for the same range of \bar{t} as in figure 2. Figure 4 shows p_{\perp} versus \bar{r} for a range of \bar{t} ($\bar{t} = 1, 2, 5, 10$), for a case where $\kappa_{\perp} \neq 0$ and $V_z = 0$ ($\alpha = 0.1$ and $\beta = 0$), whereas figure 5 shows the radial profile of P_{\perp} when both $\kappa_{\perp} \neq 0$ and $V_z \neq 0$ ($\alpha = 0.1$ and $\beta = 0.2$). The main point to note in figures 2–5 is that the solutions in figures 2 and 3 with $\kappa_{\perp} = 0$ diverge at $r = 0$. This behavior can be deduced from the solution (3.2) or equivalently from (2.64). From (3.2) the integrand

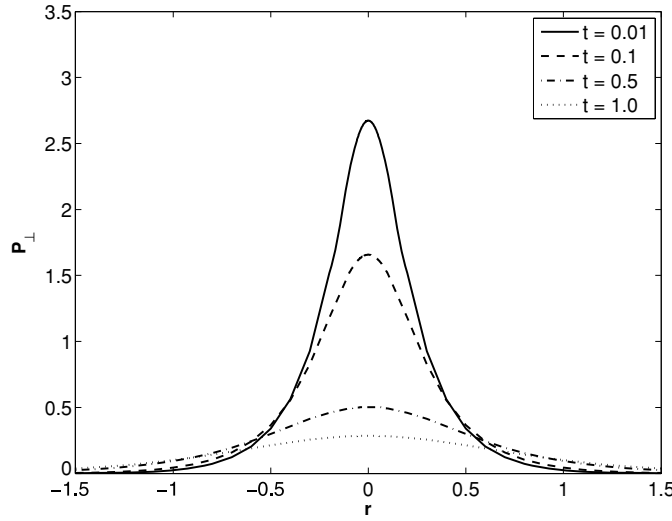


Figure 6. p_{\perp} versus \bar{r} for a range of \bar{t} ($\bar{t} = 0.01, 0.1, 0.5, 1$) using the advection–diffusion length and time scales $L_2 = \kappa_{\parallel}/V_z$ and $T_2 = \kappa_{\parallel}/V_z^2$. The parameters $\alpha = 0.1$ and $\beta = 0.2$.

has a non-integrable singularity when $\theta = -(V_z^2 t / (4\kappa_{\parallel}))^{1/2}$. This corresponds to the point $\Delta z = 0$ in (2.64). For figures 4 and 5 $\kappa_{\perp} \neq 0$ (i.e. $\beta \neq 0$), and the solution is smooth and finite at $r = 0$. Thus, local cross-field diffusion $\kappa_{\perp} \neq 0$ smooths and regularizes the solution for p_{\perp} at $r = 0$.

Figure 6 shows an example of the radial profiles of p_{\perp} , but now using the advection–diffusion length and time scales L_2 and T_2 as in (3.13) (i.e., $\bar{\kappa}_{\parallel} = 1, |\bar{V}_z| = 1, \bar{\kappa}_{\perp} = \alpha, \bar{D}_L = \beta$). The profiles are given at times $\bar{t} = 0.05, 0.1, 0.5$ and 1 . In figure 6, $\alpha = 0.1, \beta = 0.2$ (i.e., $\bar{\kappa}_{\perp} = 0.2, \bar{D}_L = 0.2$), so that advection, parallel diffusion, perpendicular diffusion and field line random walk are all operative. Figure 7 shows a three-dimensional plot of p_{\perp} versus r and t for the same parameters as in figure 6 ($\alpha = 0.1$ and $\beta = 0.2$). The figure shows a sharply peaked radial distribution for p_{\perp} at early times, which decreases in amplitude and spreads out at late times.

Figure 8 shows the variances $\langle \bar{x}^2 \rangle$ versus \bar{t} using the advection–diffusion length and time scales $L_2 = \kappa_{\parallel}/V_z$ and $T_2 = \kappa_{\parallel}/V_z^2$ for the cases (a) $\alpha = 0.1, \beta = 0.2$, (b) $\alpha = 0.1, \beta = 0$ and (c) $\alpha = 0, \beta = 0.2$. For $\alpha = 0.1, \beta = 0$, the solution for p_{\perp} is the heat equation Green’s function (3.6) with $\bar{\kappa}_p = \bar{\kappa}_{\perp} = 0.1$. The variance in this case is given by the formula $\langle \bar{x}^2 \rangle = 2\bar{\kappa}_{\perp}\bar{t}$, which is the straight line, dashed curve with least slope. The asymptotic straight line curves correspond to the expected variances $\langle \bar{x}^2 \rangle$ at late times when ordinary diffusive evolution of p_{\perp} takes place. In the late time limit, $\langle \bar{x}^2 \rangle \approx 2(\bar{\kappa}_{\perp} + \bar{\kappa}_F)\bar{t} \equiv 2(\alpha + \beta)\bar{t}$. Note that at early times the variance in these latter two cases is larger than that expected due to ordinary diffusion, and is due to the effects of compound particle transport.

4. Physical implications

The above analysis implies that the effective cross-field diffusion coefficient $\kappa_{\perp e}$ in the presence of field line random walk ($D_L \neq 0$) and advection and drift of the particles parallel to the mean magnetic field ($V_z \neq 0$) is given by

$$\kappa_{\perp e} = \kappa_{\perp} + \kappa_F, \quad \kappa_F = |V_z|D_L, \tag{4.1}$$

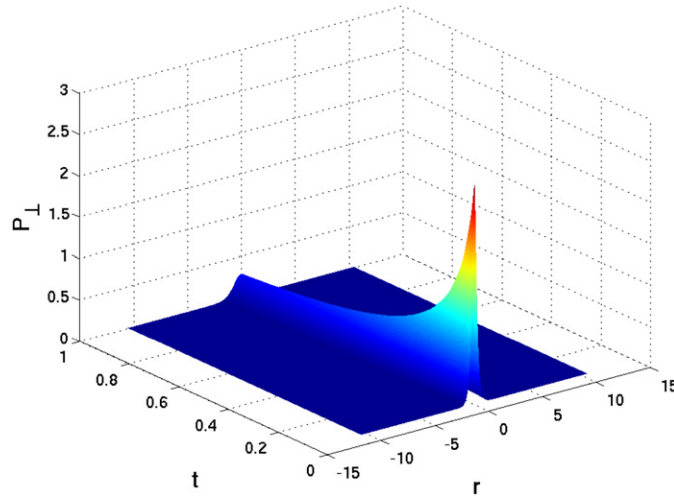


Figure 7. A three-dimensional plot of p_{\perp} versus \bar{r} and \bar{t} for the same parameters as in figure 6 ($\alpha = 0.1$ and $\beta = 0.2$). The figure shows that p_{\perp} is sharply peaked about $\bar{r} = 0$ at early times, but decreases in amplitude and spreads out in \bar{r} at late times.

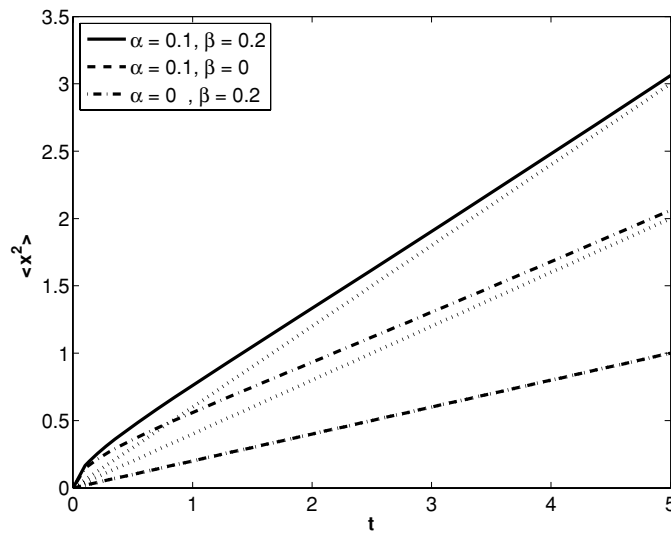


Figure 8. The mean square value of $\langle \bar{x}^2 \rangle$ versus \bar{t} using the length scale $L_2 = \kappa_{\parallel} / V_z$ and time scale $T_2 = \kappa_{\parallel} / V_z^2$ for the cases (a) $\alpha = 0.1, \beta = 0.2$ (b) $\alpha = 0.1$ and $\beta = 0$, and (c) $\alpha = 0$ and $\beta = 0.2$. Also shown is the mean-square displacement $\langle \bar{x}^2 \rangle = 2(\alpha + \beta)\bar{t}$ versus \bar{t} applicable at late times.

(see (2.72)), where κ_F is the particle diffusion coefficient due to field line random walk. This result has potential implications for models of the eleven year, solar-cycle modulation of galactic cosmic rays (e.g., Kota and Jokipii 1983, Hattingh and Burger 1995, Jokipii and Thomas 1981, Potgieter and Moraal 1985, Alanko-Huotari *et al* 2007). In (4.1),

$$V_z = (\mathbf{u} + \mathbf{V}_D) \cdot \mathbf{e}_B \tag{4.2}$$

is the effective drift velocity of the particles parallel to the mean magnetic field \mathbf{B} with unit normal $\mathbf{e}_B = \mathbf{B}/B$.

As an illustrative example of the above ideas, consider a simplified model of the interplanetary magnetic field, used in modulation models, including the effects of drifts, in which there is a flat current sheet in the helio-equatorial plane with a change of magnetic polarity across the sheet. The flat current sheet model was used by Jokipii *et al* (1977) to discuss the role of drifts on energetic charged particle transport in the heliosphere. More complicated interplanetary magnetic field configurations are in general possible. For example, Jokipii and Thomas (1981) discuss the effects of a wavy neutral sheet with tilt on the Parker spiral field. Fisk (1996) modified the Parker spiral magnetic field to take into account the off-set of the magnetic and rotational axes of symmetry at the solar source surface. However, our aim is to illustrate the basic physical implications of (4.1), and we restrict our discussion to the flat current sheet model.

For the flat current sheet model (which is a reasonable description of the field at solar minimum), the magnetic field on either side of the sheet is the Parker, Archimedean spiral magnetic field (e.g., Parker 1958). The magnetic field in this model is given by

$$\mathbf{B} = \frac{A}{r^2}(\mathbf{e}_r - \tan \psi \mathbf{e}_\phi)[1 - 2H(\theta - \pi/2)], \quad (4.3)$$

where

$$\tan \psi = \frac{\Omega r \sin \theta}{V_w}, \quad A = \sigma B_0 r_0^2, \quad \sigma = \pm 1 \quad (4.4)$$

defines the Archimedean spiral angle ψ , between \mathbf{e}_B and the radial direction; Ω is the angular frequency of rotation of the Sun and V_w is the solar wind speed (assumed to be constant and radial). Here (r, θ, ϕ) are spherical polar coordinates centered on the Sun, $\mathbf{e}_r, \mathbf{e}_\theta, \mathbf{e}_\phi$ are unit vectors in the radial, helio-latitudinal and azimuthal directions, and $H(x)$ is the Heaviside step function. In (4.3)–(4.4) $A = \sigma B_0 r_0^2$ is a constant and $\sigma = \pm 1$ (B_0 is the radial magnetic field strength at radius $r = r_0$ at the solar surface). For $\sigma = 1$, the radial magnetic field component B_r is outward in the northern hemisphere ($0 < \theta < \pi/2$) and inward below the current sheet for $\pi/2 < \theta < \pi$. The opposite polarity is obtained for $\sigma = -1$.

4.1. The drift velocity

In (4.2), the drift velocity of the particles \mathbf{V}_D due to curvature and gradient B drifts and drifts parallel to \mathbf{B} is given by

$$\mathbf{V}_D = \nabla \times (\kappa_T \mathbf{e}_B), \quad (4.5)$$

where κ_T is the anti-symmetric component of the cosmic ray diffusion tensor. In the weak scattering limit, $\kappa_T \approx vr_L/3$, where v is the particle speed, $r_L = pc/(ZeB)$ is the particle Larmor-radius, p is the particle momentum, Ze is the particle charge and c is the speed of light. From (4.5), the component of the drift velocity parallel to the magnetic field $V_{Dz} \equiv V_{D\parallel}$ is given by

$$V_{D\parallel} = \mathbf{V}_D \cdot \mathbf{e}_B = \kappa_T \frac{\nabla \times \mathbf{B} \cdot \mathbf{B}}{B^2}. \quad (4.6)$$

Thus, the field aligned component of \mathbf{V}_D depends on the field aligned current $J_{\parallel} = \nabla \times \mathbf{B} \cdot \mathbf{e}_B$, associated with the magnetic field (4.3).

For the flat current sheet model (4.3) for the magnetic field \mathbf{B} , the drift velocity \mathbf{V}_D from (4.5) in the weak scattering limit ($\kappa_T = vr_L/3$) has the form

$$\mathbf{V}_D = \mathbf{V}_D^{(m)} + \mathbf{V}_D^{(s)} \delta(\theta - \pi/2), \quad (4.7)$$

(e.g., Jokipii *et al* (1977)), where

$$\mathbf{V}_D^{(s)} = \frac{2vpcr}{3qA(1 + \tan^2 \psi)} (\mathbf{e}_\phi + \tan \psi \mathbf{e}_r) \quad (4.8)$$

is the singular component of the drift velocity in the current sheet and

$$\begin{aligned} \mathbf{V}_D^{(m)} = & \frac{2vpcr}{3qA(1 + \tan^2 \psi)^2} (-\tan \psi \cot \theta \mathbf{e}_r + \tan \psi (2 + \tan^2 \psi) \mathbf{e}_\theta \\ & + \tan^2 \psi \cot \theta \mathbf{e}_\phi) [1 - 2H(\theta - \pi/2)] \end{aligned} \quad (4.9)$$

is the mean, non-singular component of the drift velocity outside of the current sheet. Note that the non-singular component of the drift $\mathbf{V}_D^{(m)}$ and \mathbf{e}_B change sign across the current sheet. Using (4.8) we find

$$V_{D\parallel}^{(s)} = 0, \quad (4.10)$$

so that there is no contribution to $V_{D\parallel}$ from the singular current sheet component $\mathbf{V}_D^{(s)}$. Thus, from (4.9) we obtain

$$V_{D\parallel} \equiv V_{Dz} = -\frac{2vpcr \tan \psi \cot \theta}{3q|A|(1 + \tan^2 \psi)^{3/2}}, \quad (4.11)$$

for the component of the drift velocity parallel to \mathbf{B} . The drift velocity component $V_{D\parallel}$ in (4.11) can be written in the more convenient form

$$V_{Dz} = -\frac{2}{3}v \left(\frac{r_L}{r} \right) \frac{\Omega r \cos \theta}{V_w} \cos^2 \psi, \quad (4.12)$$

where

$$r_L = \frac{pc}{qB}, \quad B = \frac{|A|}{r^2} \sec \psi \quad (4.13)$$

is the particle Larmor-radius at radius r and heliolatitude θ , and $B = B(r, \theta)$ is the corresponding magnetic field strength. The form of V_{Dz} in (4.12) shows that $V_{Dz} = 0$ at the current sheet at $\theta = \pi/2$ and increases toward the poles where $\theta \rightarrow 0$. In addition, V_{Dz} scales as the particle Larmor-radius, and in general is small for low rigidity particles for which $r_L/r \ll 1$, but V_{Dz} can be significant at higher rigidities (note we require $V_{Dz} < v$ in general on physical grounds). Using (4.2), we obtain above the current sheet

$$V_z(\theta) = \sigma V_w \cos \psi + V_{Dz}(\theta), \quad (4.14)$$

where $0 \leq \theta \leq \pi/2$. Below the current sheet, we obtain

$$V_z(\pi - \theta) = -\sigma V_w \cos \psi - V_{Dz}(\theta), \quad (4.15)$$

where from (4.11), $V_{Dz}(\pi - \theta) = -V_{Dz}(\theta)$. Thus $|V_z|$ is symmetric about the current sheet. Because of the change of polarity across the current sheet, $\sigma V_w \cos \psi \rightarrow -\sigma V_w \cos \psi$ as we change from θ to $\pi - \theta$, where V_w is the radial solar wind speed. Also note that because both \mathbf{e}_B and \mathbf{V}_D change sign across the current sheet, the formula (4.11) for V_{Dz} applies both above and below the current sheet.

4.2. The field line random walk coefficient D_L

In this subsection, we discuss ways in which to estimate the field line random walk coefficient D_L . It is important to note that our analysis has assumed at the outset that the field line random walk statistics are Gaussian, with pdf P_{FRW} given by (2.9). Ragot (1999, 2001, 2006a–2006c) and Shalchi and Kourakis (2007a, 2007b) have discussed evidence that the

field line statistics, as observed by spacecraft in the inner heliosphere, may not be Gaussian, but can be subdiffusive ($\langle \Delta x^2 \rangle \propto \Delta z^\alpha$, $\alpha < 1$) or superdiffusive ($\langle \Delta x^2 \rangle \propto \Delta z^\alpha$, $\alpha > 1$) depending on the value of Δz and the spectral shape of the power spectrum tensor $P_{ij}(\mathbf{k})$ of the magnetic field fluctuations. We could in principle also develop the theory for cross-field particle transport, based on a non-Gaussian form for P_{FRW} describing the field line random walk and other particle propagators P_p in the Chapman–Kolmogorov equation (2.2) to describe the cross-field particle transport, but these generalizations will not be pursued in this paper.

Jokipii and Parker (1969) assuming slab turbulence obtained the formula

$$\begin{aligned} D_L &= \left\langle \frac{(\Delta x)^2}{2\Delta z} \right\rangle = \frac{u_0}{2B_0^2} \int_{-\infty}^{\infty} \langle \delta B_x(t) \delta B_x(t + \tau) \rangle d\tau \\ &= \frac{u_0}{2B_0^2} P_{xx}(f = 0), \end{aligned} \quad (4.16)$$

for the field line random walk coefficient D_L , where we assume cylindrical symmetry of the turbulent fluctuations about the mean magnetic field, $P_{xx}(f)$ is the power spectrum of the magnetic field fluctuations (slab turbulence) normal to the mean field at frequency f , and u_0 is the radial solar wind speed. Using Mariner spacecraft data, they obtained $D_L \sim 2.5 \times 10^{10}$ cm for the field line random walk coefficient near Earth at 1 AU (use $P_{xx}(f = 0) = 2 \times 10^4 \gamma^2 \text{ Hz}^{-1}$ ($1\gamma = 10^{-5}$ Gauss), and $B_0 = 4\gamma$, $u_0 = 350 \text{ km s}^{-1}$ in (4.16).

Matthaeus *et al* (1995) used Corsinn’s independence hypothesis to investigate field line random walk in slab plus 2D turbulence. They obtained the formula

$$D_L = \left\langle \frac{\Delta x^2}{2\Delta z} \right\rangle = \frac{1}{2} [D_{\text{slab}} + (D_{\text{slab}}^2 + 4D_{2D}^2)^{1/2}], \quad (4.17)$$

for the field line random walk coefficient D_L . Here, D_{2D} and D_{slab} are the field line random walk coefficients for 2D and slab turbulence, respectively. The result (4.17) implicitly assumes that the integral defining D_{2D} converges and is well defined. D_{2D} is related to the so-called ultra scale of the turbulence.

Assuming slab plus 2D turbulence, Shalchi *et al* (2009a) estimate that near 1 AU

$$\begin{aligned} \frac{D_{\text{slab}}}{l_{\text{slab}}} &= \pi C(\nu) \frac{\delta B_{\text{slab}}^2}{B_0^2} \approx 0.075, \\ \frac{D_{2D}}{l_{\text{slab}}} &= \sqrt{\frac{s-1}{2(q-1)}} \frac{l_{2D}}{l_{\text{slab}}} \frac{\delta B_{2D}}{B_0} \approx 0.073, \\ \frac{D_L}{l_{\text{slab}}} &\approx 0.120, \end{aligned} \quad (4.18)$$

where $C(\nu)$ is a normalization constant for the slab turbulence power spectrum and $s = 2\nu = 5/3$ is the spectral index of the turbulence in the inertial range, and we choose $q = 1.5$. Here, s and q are spectral exponents describing the 2D turbulence component, and δB_{slab} and δB_{2D} are the characteristic magnetic field fluctuations associated with the slab and 2D components of the turbulence (see appendix C for details). Taking $l_{\text{slab}} = 0.03$ AU, $l_{2D} = 0.1l_{\text{slab}}$, $B_0 = 4.12$ nT, $\delta B/B_0 = 1$, $\delta B_{\text{slab}}^2 = 0.2\delta B^2$ and $\delta B_{2D}^2 = 0.8$ (this corresponds to 20% slab and 80% 2D turbulence) $s = 5/3$ and $q = 1.5$ in (4.18) we obtain $D_L \sim 3.6 \times 10^{-3}$ AU = 5.38×10^{10} cm, which is comparable to the estimate of Jokipii and Parker (1969) above based on the Mariner data.

4.3. Perpendicular mean free paths

In this section, we give examples of the contribution of field line random walk and advection and drift to the effective cross field diffusion coefficient $\kappa_{\perp e}$ based on (4.1). We use the

estimate $D_L \sim 3.6 \times 10^{-3} \text{AU} = 5.38 \times 10^{11} \text{cm}$ for the field line random walk diffusion coefficient D_L near Earth in the following analysis.

In the solar equatorial plane ($\theta = \pi/2$), the drift velocity component V_{Dz} parallel to the Parker spiral magnetic field is zero (i.e., $V_{Dz} = 0$ in (4.11)). Hence $|V_z| = V_w \cos \psi$ is the effective advection speed parallel to \mathbf{B} . For a nominal Parker spiral field, with $V_w = 400 \text{ km s}^{-1}$ and $\psi = 45^\circ$ at Earth, we obtain $|V_z| = 282.8 \text{ km s}^{-1}$ at Earth. For these values of the parameters, the random walk, cross-field diffusion coefficient near Earth, near the current sheet is thus $\kappa_F = |V_z| D_L \sim 1.517 \times 10^{18} \text{ cm}^2 \text{ s}^{-1}$.

For $\theta \neq \pi/2$, there is a nonzero contribution to V_z from the drift V_{Dz} parallel to the Parker spiral field \mathbf{B} . In general, the effective perpendicular mean free path of the particles is given by

$$\lambda_{\perp e} = \lambda_{\perp} + \lambda_{\perp F}, \quad \lambda_{\perp} = 3 \frac{\kappa_{\perp}}{v}, \quad \lambda_{\perp F} = 3 \frac{\kappa_F}{v}, \quad (4.19)$$

where v is the particle speed and $\kappa_F = |V_z| D_L$. Using expression (4.14) for V_z we obtain

$$\lambda_{\perp F} = \frac{3V_w D_L \cos \psi |\hat{V}_z|}{\beta c}, \quad (4.20)$$

where

$$\hat{V}_z = \frac{V_z}{\sigma V_w \cos \psi} = 1 - \frac{2}{3} \sigma \left(\frac{v}{V_w} \right) \left(\frac{r_L}{r_e} \right) \left(\frac{\Omega r_e}{V_w} \right) \cos \theta \cos \psi \quad (4.21)$$

is the normalized version of V_z above the current sheet. Note $|\hat{V}_z|$ is symmetric about the current sheet (see (4.14) et seq.). The parameter $\beta = v/c$ is the ratio of the particle speed to the speed of light. It can be expressed in the form

$$\beta = \frac{v}{c} = \frac{P}{\sqrt{P^2 + P_0^2}}, \quad (4.22)$$

where

$$P = \frac{pc}{Ze}, \quad P_0 = \frac{E_0}{Ze} \quad (4.23)$$

defines the particle rigidity P and the rigidity P_0 correspond to the rest mass energy $E_0 = m_0 c^2$ of the particle. If P and P_0 are measured in MV then for electrons (e^-) and protons (H^+) we have

$$P_0 = \begin{cases} 0.511 \text{ MV} & \text{for } e^- \\ 938 \text{ MV} & \text{for } H^+. \end{cases} \quad (4.24)$$

Taking $V_w = 400 \text{ km s}^{-1}$, $D_L = 3.6 \times 10^{-3} \text{ AU}$, $c = 3 \times 10^8 \text{ m s}^{-1}$, expression (4.20) for $\lambda_{\perp F}$ reduces to

$$\lambda_{\perp F} = 1.44 \times 10^{-5} \frac{\cos \psi}{\beta} |\hat{V}_z| \text{AU}, \quad (4.25)$$

for the perpendicular mean free path $\lambda_{\perp F}$. Noting that

$$\frac{r_L}{r_e} = \frac{P}{r_e B_e (B/B_e)} = \frac{P(\text{MV})}{2.2425 \times 10^5 (B/B_e)}, \quad (4.26)$$

(i.e., $r_e B_e = 2.2425 \times 10^5 \text{ MV}$ for $r_e = 1 \text{ AU}$ and $B_e = 5 \text{ gammas} = 5 \times 10^{-5} \text{ Gauss}$) and noting that $\Omega r_e / V_w = 1.00666 \approx 1$, where $\Omega = 2.6934 \times 10^{-6} \text{ s}^{-1}$ corresponds to the rotation rate of the Sun (i.e., a rotation period of 27 days), we obtain

$$\hat{V}_z = 1 - \frac{2}{3} C_1 \sigma \frac{\beta P}{(B/B_e)} \cos \theta \cos \psi, \quad (4.27)$$

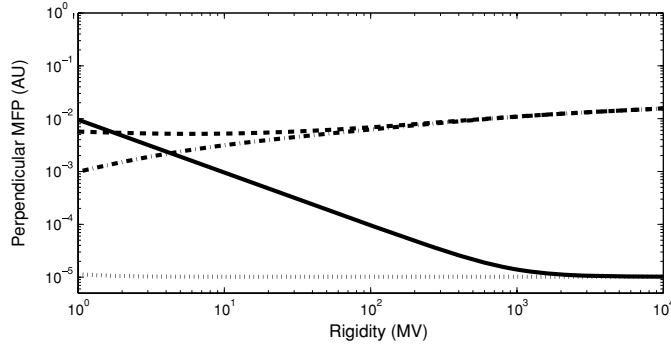


Figure 9. Perpendicular mean free paths due to field line random walk for electrons (dotted curve) and protons (solid curve) for $|V_z| = V_w \cos \psi$ near the current sheet ($\theta \sim 90^\circ$) and near Earth at 1 AU. $V_w = 400 \text{ km s}^{-1}$ and $\psi = 45^\circ$. Also shown are the perpendicular mean free paths for protons (dashed curve) and electrons (dashed-dotted curve) obtained by Shalchi and Dosch (2008) for comparison.

where $C_1 = 3.3444 \times 10^{-3}$. Thus, (4.22), (4.27) and (4.25) give the perpendicular mean free path $\lambda_{\perp F}$ due to field line random walk as a function of the particle magnetic rigidity P in MV and in terms of the geometry of the Parker spiral magnetic field. Note that $\hat{V}_z = 1$ in the solar equatorial plane when $\theta = \pi/2$ but $\hat{V}_z \neq 1$ for $\theta \neq \pi/2$ where drifts contribute to V_z .

Note in (4.27) that

$$\frac{B}{B_e} = \frac{1}{\sqrt{2} \cos \psi} \left(\frac{r_e}{r} \right)^2, \quad \cos \psi = \frac{1}{\sqrt{1 + (\Omega r \sin \theta / V_w)^2}}, \quad (4.28)$$

and hence

$$\hat{V}_z = 1 - \frac{2\sqrt{2}}{3} C_1 \sigma \frac{\beta P \cos \theta (r/r_e)^2}{1 + (\Omega r \sin \theta / V_w)^2}. \quad (4.29)$$

This latter expression for \hat{V}_z shows a complicated dependence on r and θ . In this paper, we limit our numerical examples of $\lambda_{\perp F}$ to $r = r_e = 1 \text{ AU}$. Note that in general D_L will be a function of r and θ , depending on the evolution of the turbulence throughout the heliosphere (e.g., Zank *et al* (1996)). These issues lie beyond the scope of this paper where we simply take $D_L = 3.6 \times 10^{-3} \text{ AU}$ and restrict our attention to $r = r_e = 1 \text{ AU}$.

Figure 9 shows the plots of the perpendicular mean free path due to field line random walk for both protons (solid line) and electrons (dashed curve) based on the above parameters as a function of particle rigidity. For comparison, we have also shown the perpendicular mean free paths for electrons (dashed curve) and protons (dashed-dotted curve) obtained by Shalchi and Dosch (2008). The latter results were obtained by combining the nonlinear guiding center theory for cross-field diffusion with the Lorentz force equation (see also Shalchi *et al* (2009a)). Both electrons (dotted curve) and protons (solid curve) show an increase in $\lambda_{\perp F}$ at low rigidities. However, the proton rigidities should not be extended below about 1.2 MV, which corresponds to a proton moving at the solar wind speed (i.e., $v = V_{sw} = 400 \text{ km s}^{-1}$). At high rigidities, there is no effective contribution to the total λ_{\perp} .

Figures 10 and 11 show the perpendicular mean free paths $\lambda_{\perp F}$ for protons at helio co-latitudes of $\theta = 0, \pi/4$ and $\pi/2$. Note that $\lambda_{\perp F}$ is symmetric about the current sheet. In figure 10, $\sigma = -1$ corresponds to a configuration in which the radial magnetic field is inward above the current sheet and outward below the current sheet. Note that $\theta = \pi/2$ corresponds to

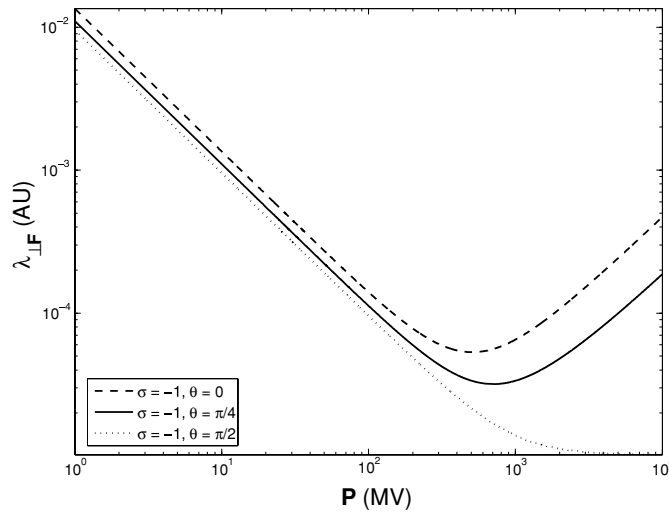


Figure 10. Perpendicular mean free paths for protons due to field line random walk for an interplanetary field configuration with $\sigma = -1$ (radial field inward above the current sheet). $\theta = 0, \pi/4$ and $\pi/2$.

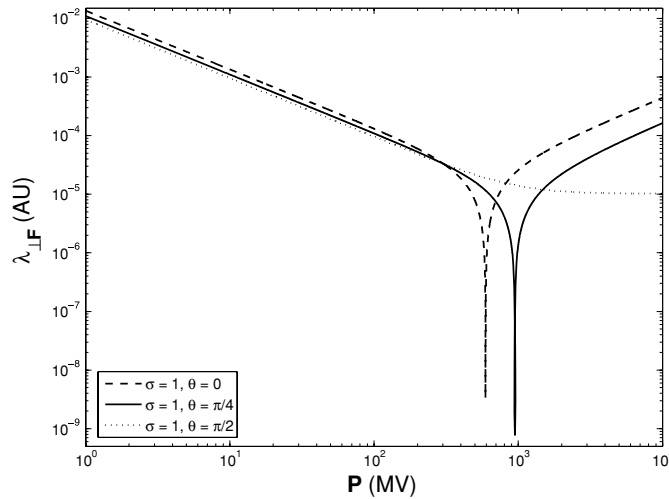


Figure 11. Perpendicular mean free path $\lambda_{\perp F}$ for protons due to field line random walk for an interplanetary field configuration with $\sigma = 1$ (radial field outward above the current sheet). $\theta = 0, \pi/4$ and $\pi/2$.

a position in the current sheet at the helio-equator and $\theta = 0$ corresponds to over the poles. For the case $\sigma = -1$, there is an enhancement in $\lambda_{\perp F}$ due to the drifts (note that the effective drift velocity V_{Dz} does not contain the singular current sheet drift; the drifts are the non-singular component of the drift parallel to \mathbf{B}). There is an increase in $\lambda_{\perp F}$ at large rigidities due to drifts. In figure 11, $\sigma = 1$. In this latter case, there is a rigidity $P = P_*$ ($P_* \approx 10^3$ MV) where $\lambda_{\perp F} = 0$, since the advection and effective drift velocities are in opposite directions below this rigidity. There is a significant contribution to $\lambda_{\perp F}$ above $P = P_*$. Similar variations for $\lambda_{\perp F}$

for $\sigma = \pm 1$ also occur for the electrons (not shown). The effect of drifts on $\lambda_{\perp F}$ is maximal over the poles where $\theta = 0$.

It is important to keep in mind the basic limitations to the theory used in the derivation of the FLRW diffusion coefficient κ_F . In particular, the integral along the field line over z in the Chapman–Kolmogorov equation (2.2) should be over many correlation scales, but not over such a large scale as to violate the assumption that V_{sw} , B , κ_{\parallel} and κ_{\perp} are approximately constant used in the particle propagator P_p . To estimate these limitations, we note from (4.26) that $r_L/r_e \sim 0.05$ AU for a $P = 10^4$ MV particle in the vicinity of Earth at $r = 1$ AU. If the averaging length L_{av} used in the Chapman–Kolmogorov equation (2.2) was 10 Larmor radii say, this would correspond to a distance of $L_{av} = 0.5$ AU for a 10^4 MV particle. The application of the theory in this case would be marginal. However, for $P = 10^3$ MV, $r_L/r_e \sim 0.005$ AU, and the assumptions of the theory would be fulfilled.

5. Conclusions

In this paper, we have developed the Chapman–Kolmogorov equation approach to compound cross-field diffusion, in which the probability distribution function (pdf) for cross-field transport, P_{\perp} , is given as a convolution of the pdf for field line random walk, P_{FRW} , and the pdf for particle transport, P_p , relative to the random walking magnetic field. The analysis was restricted to the case of normal diffusive field line random walk for P_{FRW} (this restriction could in general be relaxed in more general models). The pdf for particle transport, P_p , took into account advection, drift, parallel diffusion and local cross-field diffusion.

The mean square deviation (MSD) of the particle for crossing the field $\langle \Delta x^2(t) \rangle$ was obtained by taking moments of the pdf P_{\perp} . At early times, $\langle \Delta x^2(t) \rangle \propto \sqrt{t}$ characteristic of compound diffusion (e.g., Kota and Jokipii (2000), Webb *et al* (2006, 2008)), whereas at late times $\langle \Delta x^2(t) \rangle \sim 2(\kappa_{\perp} + \kappa_F)t$, where κ_{\perp} is the local cross-field diffusion coefficient and $\kappa_F = |V_z|D_L$ is the cross-field diffusion coefficient due to field line random walk (D_L) and due to drift and advection parallel to the mean field ($|V_z|$). The long time diffusive behavior is obtained on a time scale of a few advection–diffusion times scales $T_2 = \kappa_{\parallel}/V_z^2$ where κ_{\parallel} is the parallel diffusion coefficient. A method for determining the higher order moments of the pdf P_{\perp} was developed (appendix A) and was used to obtain explicit formulae for the fourth-order moments.

Numerical examples of the pdf P_{\perp} were obtained (figures 2–7). In the absence of local cross-field diffusion ($\kappa_{\perp} = 0$), the distributions exhibit a logarithmic divergence with cylindrical distance r as the source field line is approached (figures 2 and 3). This includes the case of compound diffusion ($\kappa_{\perp} = 0$ and $V_z = 0$), for which the pdf P_{\perp} can be expressed in terms of a Meijer G function (appendix B). For cases with $\kappa_{\perp} \neq 0$, the pdfs have a smooth bell-shaped profile with cylindrical radius about the source field line (figures 4–7).

Estimates of the cross-field diffusion coefficient $\kappa_F = |V_z|D_L$ due to field line random walk and advection and drift were obtained for a model with an Archimedean, Parker spiral magnetic field, in which the field changes polarity across a flat current sheet located in the solar equatorial plane. The field line random walk coefficient D_L was estimated for slab plus 2D turbulence power spectra, by using the results of Matthaeus *et al* (1995), Shalchi and Kourakis (2007a, 2007b) and Shalchi *et al* (2009a). Estimates of κ_F were obtained both near the current sheet ($\theta \approx 90^\circ$) and at higher heliolatitudes ($\theta = 45^\circ$ and $\theta = 0^\circ$). Near the current sheet ($\theta \approx 90^\circ$), the effective advection speed $|V_z| = V_w \cos \psi$, where V_w is the solar wind speed and ψ is the interplanetary spiral field angle (there is no effective contribution to $|V_z|$ from drifts in this case). The effects of particle drifts on $\lambda_{\perp F}$ are maximal over the poles (Figures 10 and 11). The perpendicular mean free path $\lambda_{\perp} = 3\kappa_{\perp}/v$ obtained in a recent model of

perpendicular diffusion based on the generalized NLGC–Newton–Lorentz theory of Shalchi and Dosch (2008) was compared with the field line random walk contribution $\lambda_{\perp F} = 3\kappa_F/v$. It was found that there can be a substantial contribution to the total perpendicular mean free path $\lambda_{\perp e} = \lambda_{\perp} + \lambda_{\perp F}$ due to field line random walk at low rigidities (Figure 9: see also Shalchi *et al* (2009a)).

The Chapman–Kolmogorov approach to cross-field particle transport used in this paper was restricted to the case of normal diffusive field line random walk. This restriction of the theory can clearly be relaxed to take into account the possibility of subdiffusive or superdiffusive field line random walk, by using a modified pdf P_{FRW} for the field line random walk. Shalchi *et al* (2009b) have used a kappa distribution for the field line random walk pdf. They obtain results that are similar to using a Gaussian pdf for the field line random walk. The pdf P_p used to describe the particle transport relative to the random walking field could in principle be modified to reflect more accurately the particle transport (as determined, for example, from numerical simulations).

Acknowledgments

GMW and GPZ were supported in part by NASA grants NN05GG83G and NSF grant nos ATM-03-17509 and ATM-04-28880. EK was supported in part by NASA grants NNG05GM57G and NSF grants: ATM-0427754 and ATM-0639658. JAIR was supported in part by NASA grant NNX07AI64G. GL was supported in part by NASA grants NNG04GF83G and NNG05GH38G. A Shalchi was supported in part by the Deutsche Forschungsgemeinschaft (DFG) and under the Junges Kolleg program of the Nordrhein-Westfälische Akademie der Wissenschaften.

Appendix A

A method for calculating the moments $\langle \tilde{r}^n \rangle$ for both odd and even n is described below. By using the integral (2.64) for $P_{\perp}(\tilde{r}, t)$ in (2.65), interchanging the order of the \tilde{r} and z integrations and carrying out the integrations over \tilde{r} gives the formula

$$\langle \tilde{r}^n \rangle = 2^n \Gamma\left(\frac{n}{2} + 1\right) \int_{-\infty}^{\infty} \frac{d\Delta z}{\sqrt{4\pi\kappa_{\parallel}\Delta t}} \lambda^{n/2} \exp\left(-\frac{(\Delta z - V_z\Delta t)^2}{4\kappa_{\parallel}\Delta t}\right), \quad (\text{A.1})$$

where

$$\lambda = \kappa_{\perp}\Delta t + D_L|\Delta z|. \quad (\text{A.2})$$

By splitting the integral over Δz in (A.1) into the $\Delta z < 0$ and $\Delta z > 0$ regions, we obtain

$$\langle \tilde{r}^n \rangle = 2^n \Gamma\left(\frac{n}{2} + 1\right) (\mathcal{I}_n^- + \mathcal{I}_n^+), \quad (\text{A.3})$$

where

$$\mathcal{I}_n^{\pm} = \frac{1}{\sqrt{\pi}} \int_{w_{\pm}}^{\infty} (a_{\pm}\Delta t + b\sqrt{\Delta t}w)^{n/2} \exp(-w^2) dw, \quad (\text{A.4})$$

$$a_{\pm} = \kappa_{\perp} \pm D_L V_z, \quad b = 2D_L\sqrt{\kappa_{\parallel}}, \quad w_{\pm} = \mp \frac{V_z\sqrt{\Delta t}}{2\sqrt{\kappa_{\parallel}}}. \quad (\text{A.5})$$

By noting that

$$a_{\pm}\Delta t + b(\Delta t)^{1/2} = \kappa_{\perp}\Delta t + b(\Delta t)^{1/2}(w - w_{\pm}), \quad (\text{A.6})$$

we obtain the alternative formulae

$$\mathcal{I}_n^\pm = \frac{1}{\sqrt{\pi}} \int_{w_\pm}^\infty [\kappa_\perp \Delta t + b\sqrt{\Delta t}(w - w_\pm)]^{n/2} \exp(-w^2) dw, \quad (\text{A.7})$$

for \mathcal{I}_n^\pm .

For the even order moments, $n = 2m$ (m integer), the integrals (A.7) can be evaluated by using the Binomial theorem to expand the $\lambda^{n/2}$ term in (A.1) or (A.7) to obtain

$$\mathcal{I}_{2m}^\pm = \frac{1}{2} \sum_{s=0}^m \frac{(\kappa_\perp \Delta t)^{m-s}}{(m-s)!} (b\Delta t^{1/2})^s i^s \operatorname{erfc}(w_\pm), \quad (\text{A.8})$$

where

$$i^s \operatorname{erfc}(z) = \frac{2}{\pi^{1/2}} \int_z^\infty \frac{(t-z)^s}{s!} \exp(-t^2) dt \quad (\text{A.9})$$

are the iterated integrals of the complementary error function (Abramowitz and Stegun (1965), formula 7.2.3, p 299). We note, for later use, that

$$\begin{aligned} i^0 \operatorname{erfc}(z) &= \operatorname{erfc}(z), & i^1 \operatorname{erfc}(z) &= \frac{1}{\sqrt{\pi}} \exp(-z^2) - z \operatorname{erfc}(z), \\ i^2 \operatorname{erfc}(z) &= -\frac{z}{2\sqrt{\pi}} \exp(-z^2) + \left(\frac{1}{4} + \frac{z^2}{2}\right) \operatorname{erfc}(z). \end{aligned} \quad (\text{A.10})$$

As an application of formulae (A.3) and (A.8) for \mathcal{I}_{2m}^\pm , consider the case $m = 1$. Using the results (A.10) we obtain $\langle \tilde{x}^2 \rangle = \langle \tilde{y}^2 \rangle = \frac{1}{2} \langle \tilde{r}^2 \rangle$, where

$$\begin{aligned} \langle \tilde{x}^2 \rangle &= 2(\mathcal{I}_2^- + \mathcal{I}_2^+) \\ &= 2\kappa_\perp \Delta t + 2D_L V_z \Delta t \operatorname{erf}\left(\frac{V_z \Delta t^{1/2}}{2\kappa_\parallel^{1/2}}\right) + 4\left(\frac{\kappa_\parallel D_L^2 \Delta t}{\pi}\right)^{1/2} \exp\left(-\frac{V_z^2 \Delta t}{4\kappa_\parallel}\right), \end{aligned} \quad (\text{A.11})$$

for the nonzero, second-order moments of $P_\perp(\tilde{r}, t)$. Equations (A.11) are the second-order moments of P_\perp discussed in (2.69) in the text.

Appendix B

In this appendix, we discuss the compound diffusion solution (3.7). Because the integrand is even in θ , it can be written in the form

$$p_\perp = \int_0^\infty f(\theta) d\theta, \quad (\text{B.1})$$

where

$$f(\theta) = \frac{A}{\theta} \exp\left(-\theta^2 - \frac{B}{\theta}\right), \quad (\text{B.2})$$

$$A = \frac{1}{4\pi^{3/2} \bar{D}_L (\bar{\kappa}_\parallel \bar{t})^{1/2}}, \quad B = \frac{\bar{r}^2}{8\bar{D}_L (\bar{\kappa}_\parallel \bar{t})^{1/2}}. \quad (\text{B.3})$$

In the numerical integration of (B.1), it is useful to note that $f(\theta)$ has a maximum when $f'(\theta) = 0$, where

$$f'(\theta) = f(\theta) \frac{(B - \theta - 2\theta^3)}{\theta^2}. \quad (\text{B.4})$$

The required real root $\theta = \theta_1$ of the cubic equation obtained when $f'(\theta) = 0$ is given by

$$\theta_1 = \left[\frac{B}{4} + \left(\frac{B^2}{16} + \frac{1}{6^3} \right)^{1/2} \right]^{1/3} - \left[\left(\frac{B^2}{16} + \frac{1}{6^3} \right)^{1/2} - \frac{B}{4} \right]^{1/3}. \quad (\text{B.5})$$

For small B ($|B| \ll 1$), $\theta_1 \approx B$ and $f(\theta)$ is sharply peaked about $\theta = \theta_1$. Using Mathematica (R Burrows, personal communication (2009)), one can identify p_\perp with the Meijer G function

$$p_\perp = \frac{A}{2\sqrt{\pi}} G_{0,3}^{3,0} \left(\frac{B^2}{4} \middle| \begin{matrix} \{ \} \\ (0, 0, 1/2) \end{matrix} \right). \quad (\text{B.6})$$

Either by differentiating (B.1) multiple times or using the results from Erdelyi *et al* (1953) (*Higher Transcendental Functions* vol 1, p 206, section 5.3) one can show that p_\perp satisfies the third-order differential equation

$$\left(\delta^3 - \frac{1}{2} \delta^2 + z \right) p_\perp = 0, \quad (\text{B.7})$$

where $z = B^2/4$ and $\delta = z d/dz$. Investigation of the solutions of (B.7) about $z = 0$ reveals that $z = 0$ is a regular singular point of the differential equation in the sense that the indicial equation $\lambda^2(\lambda - 1/2) = 0$ is well defined (i.e., look for solutions with $p_\perp \propto z^\lambda$). This implies that (B.7) has three independent solutions of the form $p_\perp \sim a_1 \ln(z)$, $a_2 z^0$, $a_3 \sqrt{z}$ near $z = 0$. For the integral (B.1) for p_\perp one can show that

$$p_\perp \sim -A \ln B = -\frac{1}{4\pi^{3/2} (\bar{D}_L^2 \bar{k}_\parallel \bar{t})^{1/2}} \ln \left(\frac{\bar{r}^2}{8(\bar{k}_\parallel \bar{D}_L^2 \bar{t})^{1/2}} \right), \quad (\text{B.8})$$

for small B (i.e. for small r). This asymptotic form is to the lowest order the same as in Webb *et al* (2006) equation (3.28). In Webb *et al* (2006), the solution for p_\perp is expressed as an inverse Laplace transform.

Appendix C

In this appendix, we list analytical formulae derived by Shalchi and Kourakis (2007a) and Shalchi *et al* (2009) used to derive the results (4.18) for D_{slab} , D_{2D} and D_L given in section 4. For slab plus 2D turbulence, the power spectrum of the slab and 2D components of the turbulence have the form

$$P_{xx}^{\text{slab}} = g^{\text{slab}}(k_\parallel) \frac{\delta(k_\perp)}{k_\perp}, \quad (\text{C.1})$$

$$P_{lm}^{2D}(\mathbf{k}) = g^{2D}(k_\perp) \frac{\delta(k_\parallel)}{k_\perp} \left(\delta_{lm} - \frac{k_l k_m}{k^2} \right), \quad l, m, = x, y. \quad (\text{C.2})$$

The slab spectrum $g^{\text{slab}}(k_\parallel)$ is given by

$$g^{\text{slab}}(k_\parallel) = \frac{C(\nu)}{2\pi} l_{\text{slab}} \delta B_{\text{slab}}^2 [1 + (k_\parallel l_{\text{slab}})^2]^{-\nu}, \quad (\text{C.3})$$

where

$$C(\nu) = \frac{\Gamma(\nu)}{2\sqrt{\pi}\Gamma(\nu - 1/2)} \equiv \frac{1}{2B(1/2, \nu - 1/2)} \quad (\text{C.4})$$

is the normalization constant for the spectrum, chosen such that $\int P_{xx}^{\text{slab}}(\mathbf{k}) d^3k = \delta B_{\text{slab}}^2$. Here, $\Gamma(\nu)$ is the Gamma function and $B(p, q)$ is the Beta function (Abramowitz and Stegun (1965), chapter 6, p 255). The 2D power spectrum is taken of the form

$$g^{2D}(k_{\perp}) = A(s, q) \delta B_{2D}^2 l_{2D} \frac{(k_{\perp} l_{2D})^q}{[1 + (k_{\perp} l_{2D})^2]^s}, \quad (\text{C.5})$$

where

$$A(s, q) = \frac{2}{\pi D(s, q)}, \quad (\text{C.6})$$

$$D(s, q) = \frac{\Gamma[(s+q)/2]}{2\Gamma[(s-1)/2]\Gamma[(q+1)/2]} \equiv \frac{1}{2B[(s-1)/2, (q+1)/2]}.$$

Shalchi and Kourakis (2007a) show that for slab turbulence with power spectrum P_{xx}^{slab} as above $\langle \Delta x^2 \rangle = 2D_{\text{slab}}|z|$, where

$$D_{\text{slab}} = \pi C(\nu) l_{\text{slab}} \frac{\delta B_{\text{slab}}^2}{B_0^2}, \quad (\text{C.7})$$

(this result would be different for a different power spectrum in the energy range: Shalchi and Kourakis (2007b)). Similarly, for pure 2D turbulence: $\langle \Delta x^2 \rangle = 2D_{2D}|z|$ with $q > 1$ (Shalchi and Weinhorst (2009), Shalchi *et al* (2009)) one obtains

$$D_{2D} = \sqrt{\frac{(s-1)}{2(q-1)}} l_{2D} \frac{\delta B_{2D}}{B_0}. \quad (\text{C.8})$$

For $0 < q < 1$ and for $\langle \Delta x^2 \rangle \gg 2l_{2D}^2$, one obtains superdiffusive field line random walk, with

$$\langle \Delta x^2 \rangle = A|z|^{4/3}, \quad (\text{C.9})$$

where

$$A = 2 \left[\frac{(3+q)^2}{4(1-q)} \right]^{2/(q+3)} \left[D(s, q) \Gamma\left(\frac{q+1}{2}\right) l_{2D}^{q+1} \frac{\delta B_{2D}^2}{B_0^2} \right]^{2/(q+3)}. \quad (\text{C.10})$$

References

- Abramowitz M and Stegun I A 1965 *Handbook of Mathematical Functions* (New York: Dover)
- Alanko-Huotari K, Usoskin I G, Mursula K and Kovaltsov G A 2007 Stochastic simulation of cosmic ray modulation including a wavy heliospheric current sheet *J. Geophys. Res.* **112** A08101
- Barghouty A F and Jokipii J R 1996 Turbulent diffusion of magnetic field lines in astrophysical plasmas *Astrophys. J.* **470** 858
- Bieber J W, Wanner W and Matthaeus W H 1996 Dominant two-dimensional solar wind turbulence and implications for cosmic ray transport *J. Geophys. Res.* **101** 2511
- Burger R A, Moraal H and Webb G M 1985 Drift theory of charged particles in electric and magnetic fields *Astrophys. Space Sci.* **116** 107–29
- Chuvilgin L G and Ptuskin V S 1993 Anomalous diffusion of cosmic rays across the magnetic field *Astron. Astrophys.* **279** 278
- Chuychai P, Ruffolo D, Matthaeus W H and Rowlands G 2005 Suppressed diffusive escape of topologically trapped magnetic field lines *Astrophys. J. Lett.* **633** L49–52
- Corsinn S 1959 Atmospheric diffusion and air pollution *Advances in Geophysics* ed F Frenkiel and P Sheppard (New York: Academic) p 161
- Dolginov A Z and Toptygin I N 1967 Diffusion of cosmic particles in the interplanetary medium *Geomagn. Aeron.* **7** 785–90
- Dolginov A Z and Toptygin I N 1968 Cosmic rays in the interplanetary magnetic fields *Icarus* **8** 54–61
- Earl J A, Jokipii J R and Morfill G E 1988 Cosmic ray viscosity *Astrophys. J. Lett.* **331** L91

- Erdelyi A, Magnus W, Oberhettinger F and Tricomi G 1954 *Tables of Integral Transforms* vols 1 and 2 (New York: McGraw-Hill)
- Erdelyi A, Magnus W, Oberhettinger F and Tricomi G 1953 *Higher Transcendental Functions* vol 1 (New York: McGraw-Hill)
- Forman M A, Jokipii J R and Owens A J 1974 Cosmic ray streaming perpendicular to the mean magnetic field *Astrophys. J.* **192** 535–40
- Fisk L A 1996 Motion of the footpoints of heliospheric magnetic field lines at the Sun: implications for recurrent energetic particle events at high heliographic latitudes *J. Geophys. Res.* **101** 15547–54
- Gardiner C W 1985 *Handbook of Stochastic Methods (for physics, chemistry and the natural sciences)* 2nd edn (Berlin: Springer)
- Giacalone J and Jokipii J R 1999 Transport of cosmic rays across a turbulent magnetic field *Astrophys. J.* **520** 204
- Giacalone J, Jokipii J R and Mazur J E 2000 Small scale gradients and large scale diffusion of charged particles in the heliospheric magnetic field *Astrophys. J.* **532** L75–78
- Gleeson L J and Axford W I 1967 Cosmic rays in the interplanetary medium *Astrophys. J. Lett.* **149** L115
- Hall D E and Sturrock P A 1967 Diffusion, scattering and acceleration of particles by stochastic electromagnetic fields *Phys. Fluids* **10** 2620–8
- Hasselmann K and Wibberenz G 1968 Scattering of charged particles by random electromagnetic fields *Z. Geophys.* **34** 353
- Hattingh M and Burger R A 1995 Some properties of a fully three-dimensional drift model for the modulation of galactic cosmic rays (*24th Int. Cosmic Ray Conf.* vol 4) ed N Iucci and E Lamanna (London: International Union of Pure and Applied Physics) p 337
- Isichenko M B 1991a Effective plasma heat conductivity in a braided magnetic field: I. Quasi-linear limit *Plasma Phys. Control. Fusion* **33** 795–807
- Isichenko M B 1991b Effective plasma heat conductivity in a braided magnetic: II. Percolation Limit *Plasma Phys. Control. Fusion* **33** 809–26
- Jokipii J R 1966 Cosmic-ray propagation: I. Charged particles in a random magnetic field *Astrophys. J.* **146** 480
- Jokipii J R and Parker E N 1970 On the convection, diffusion, and adiabatic deceleration of cosmic rays in the solar wind *Astrophys. J.* **160** 735
- Jokipii J R 1971 Propagation of cosmic rays in the solar wind *Rev. Geophys. Space Phys.* **9** 27
- Jokipii J R 1973 The rate of separation of magnetic lines of force in a random magnetic field *Astrophys. J.* **183** 1029–36
- Jokipii J R and Parker E N 1969 Cosmic-ray life and the stochastic nature of the galactic magnetic field *Astrophys. J.* **155** 799
- Jokipii J R, Levy E H and Hubbard W B 1977 Effects of particle drift on cosmic ray transport: I. General properties, application to solar modulation *Astrophys. J.* **213** 861–8
- Jokipii J R and Davila J M 1981 Effects of particle drift on the transport of cosmic rays: IV. More realistic diffusion coefficients *Astrophys. J.* **248** 1156–61
- Jokipii J R and Thomas B 1981 Effects of drift on the transport of cosmic rays: IV. Modulation by a wavy interplanetary current sheet *Astrophys. J.* **243** 1115–22
- Kaghshvili E Kh, Zank G P and Webb G M 2006 Propagation of energetic charged particles in the solar wind: effects of intermittency *Astrophys. J.* **636** 1145–50
- Kota J 1979 Drift—the Essential Process in Losing Energy *16th Int. Cosmic Ray Conf. vol 3 Published by the Institute for Cosmic Ray Research, University of Tokyo, 3-2-1, Midori-cho Tanashi, Tokyo 18 Japan* ed S Miyake (London: International Union of Pure and Applied Physics) p 13 LCCN: 80-502341
- Kota J and Jokipii J R 1983 Effects of drift on the transport of cosmic rays: VI. A three-dimensional model including diffusion *Astrophys. J.* **265** 573–81
- Kota J and Jokipii J R 2000 Velocity correlation and spatial diffusion coefficients of cosmic rays: compound diffusion *Astrophys. J.* **531** 1067–70
- Krommes J A, Oberman C and Kleva R G 1983 Plasma transport in stochastic magnetic fields: part 3. Kinetics of test particle diffusion *J. Plasma Phys.* **30** 11–56
- Krymsky G F 1964 *Geomagn. Aeron.* **4** 977
- Mace R L, Matthaeus W H and Bieber J W 2000 Numerical investigation of perpendicular diffusion of charged test particles in weak magnetostatic slab turbulence *Astrophys. J.* **538** 192
- Matthaeus W H, Gray P C, Pontius D H Jr and Bieber J W 1995 Spatial structure and field-line diffusion in transverse magnetic turbulence *Phys. Rev. Lett.* **75** 2136–9
- Matthaeus W H, Qin G, Bieber J W and Zank G P 2003 Nonlinear collisionless perpendicular diffusion of charged particles *Astrophys. J. Lett.* **590** L53–56
- Mazur J E, Mason G M, Dwyer J R, Giacalone J, Jokipii J R and Stone E C 2000 Interplanetary magnetic field mixing deduced from impulsive flare particles *Astrophys. J.* **532** L79

- Parker E N 1958 Dynamics of the interplanetary gas and magnetic fields *Astrophys. J.* **128** 664
- Parker E N 1965 The passage of energetic particles through interplanetary space *Planet. Space Sci.* **13** 9
- Potgieter M S and Moraal H 1985 A drift model for the modulation of galactic cosmic rays *Astrophys. J.* **294** 425–40
- Qin G, Matthaeus W H and Bieber J W 2002a Subdiffusive transport of charged particles perpendicular to the mean magnetic field *Geophys. Res. Lett.* **29** 1048 (1.01029/2001GL014305)
- Qin G, Matthaeus W H and Bieber J W 2002b Perpendicular transport of particles in composite model turbulence: recovery of diffusion *Astrophys. J.* **578** L117–120
- Qin G, Matthaeus W H and Bieber J W 2003 Transport in random magnetic fields: diffusion, subdiffusion and nonlinear second diffusion *Solar Wind 10 Proc. 10th Int. Solar Wind Conf.* ed M Velli, R Bruno and F Malara pp 664–7
- Ragot B R 1999 On the quasilinear transport of magnetic field lines *Astrophys. J.* **525** 524–32
- Ragot B R 2001 Anomalous transport of magnetic field lines in quasilinear regime: analytical expressions *Proc. 27th Int. Cosmic Ray Conf., Hamburg, Germany* (London: International Union of Pure and Applied Physics) p 3293
- Ragot B R 2006a Mean cross-field displacement of magnetic field lines: full nonlinear calculation and comparison with generalized quasi-linear results in the solar wind *Astrophys. J.* **644** 622–30
- Ragot B R 2006b Quasi-linear magnetic field lines: anomalous transport and self-similarity, from the analytic to the numerical *Astrophys. J.* **645** 1169–79
- Ragot B R 2006c Mean cross-field displacement of magnetic field lines in slow solar wind: a confirmation of the supradiffusion predicted by the generalized quasilinear theory *Astrophys. J.* **647** 630–7
- Ragot B R 2009 Dispersal of magnetic field lines: nonlinear statistical theory and application to the slow solar wind *Astrophys. J.* **690** 619–43
- Rechester A B and Rosenbluth M N 1978 Electron heat transport in a Tokamak with destroyed magnetic surfaces *Phys. Rev. Lett.* **40** 38–41
- Ruffolo D, Matthaeus W H and Chuychai P 2003 Trapping of solar energetic particles by the small scale topology of solar wind turbulence *Astrophys. J.* **597** L169–172
- Ruffolo D, Matthaeus W H and Chuychai P 2004 Separation of magnetic field lines in 2-component turbulence *Astrophys. J.* **614** 420–34
- Ruffolo D, Chuychai P and Matthaeus W H 2006 Random walk of magnetic field lines in nonaxisymmetric turbulence *Astrophys. J.* **644** 971–80
- Schlickeiser R 2001 *Cosmic Ray Astrophysics* (Berlin: Springer)
- Skilling J 1975 Cosmic ray streaming-I effect of Alfvén waves on particles *Mon. Not. R. Astron. Soc.* **172** 557
- Shalchi A 2005 Time-dependent transport and subdiffusion of cosmic rays *J. Geophys. Res.* **110** A09103 (doi:10.1029/2005JA011214)
- Shalchi A, Bieber J W and Matthaeus W H 2004 Analytic forms of the perpendicular diffusion coefficient in magnetostatic turbulence *Astrophys. J.* **604** 675–86
- Shalchi A and Kourakis I 2007a Analytical description of stochastic field-line wandering in magnetic turbulence *Phys. Plasmas* **14** 092903-092903-6
- Shalchi A and Kourakis I 2007b Random walk of magnetic field-lines for different values of the energy range spectral index *Phys. Plasmas* **14** 112901-112901-6
- Shalchi A, Tautz R C and Schlickeiser R 2007 Field line wandering and perpendicular scattering of charged particles in Alfvénic slab turbulence *Astron. Astrophys.* **475** 415–20
- Shalchi A and Dosch A 2008 Nonlinear guiding center theory of perpendicular diffusion: derivation from the Newton–Lorentz equation *Astrophys. J.* **685** 971
- Shalchi A, Webb G M, le Roux J A and Zank G P 2009a Compound transport of charged particles with drift, advection, wave propagation effects, and an arbitrary turbulence spectrum *Astrophys. Space Sci.* (online, doi:10.1007/s10509-009-0021y)
- Shalchi A, le Roux J A, Webb G M and Zank G P 2009b Field line random walk for non-Gaussian statistics *J. Phys. A: Math. Theor.* (at press)
- Shalchi A and Weinhorst B 2009 Random walk of magnetic field lines: sub-diffusive, diffusive and super-diffusive regimes *Adv. Space Res.* **43** 1429–35
- Sokolov I M, Klafter J and Blumen A 2002 Fractional kinetics *Phys. Today* **55** 48–55
- Webb G M 1985 Relativistic transport theory for cosmic rays *Astrophys. J.* **296** 319–30
- Webb G M 1989 The diffusion approximation and transport theory for cosmic rays in relativistic flows *Astrophys. J.* **340** 1112–23
- Webb G M and Gleeson L J 1979 On the equation of transport for cosmic-ray particles in the interplanetary region *Astrophys. Space Sci.* **60** 335–51
- Webb G M, Martinic N J and Moraal H 1981 Scatter free propagation and drifts of cosmic-rays in the heliosphere *17th Int. Cosmic Ray Conf., Paris* vol 10 p 109–12 (A82-30442 14-88) (Gif-sur-Yvette, Essonne, France: Commissariat à l’Énergie Atomique, 1982)

- Webb G M, Zank G P, Kaghshvili E Kh and le Roux J A 2006 Compound and perpendicular diffusion of cosmic rays and random walk of the Field lines: I. Parallel particle transport models *Astrophys. J.* **651** 211–36
- Webb G M, Le Roux J A, Zank G P, Kaghshvili E Kh and Li G 2008 Compound perpendicular diffusion of cosmic rays and Field line random walk, with drift, *Particle Acceleration and Transport in the Heliosphere and Beyond: 7th Ann. Int. (Astrophysics Conf., AIP Conf. Proc. vol 1039)*, pp 246–51
- Zank G P, Matthaeus W H and Smith C W 1996 Evolution of turbulent magnetic fluctuation power with heliospheric distance *J. Geophys. Res.* **101** 17093–108
- Zank G P, Gang L, Florinski V, Matthaeus W H, Webb G M and le Roux J A 2004 Perpendicular diffusion coefficient for charged particles of arbitrary energy *J. Geophys. Res.* **109** A04107 (doi:10.1029/2003JA010301)
- Zimbardo G P, Veltri P and Pommois P 2000 Anomalous, quasilinear and percolative regimes for magnetic field line transport in axisymmetric turbulence *Phys. Rev. E* **61** 1940-48
- Zimbardo G, Pommois P and Veltri P 2004 Magnetic flux tube evolution in solar wind magnetic turbulence *J. Geophys. Res.* **109** A02113 (doi:10.1029/2003JA010162)